Mapping local green hydrogen cost-potentials by a multidisciplinary approach

S. Ishmam [a,b], H. Heinrichs [a,*], C. Winkler [a,b], B. Bayat [c,d], A. Lahnaoui [a], S. Agbo [f],
E.U. Pena Sanchez [a,b], D. Franzmann [a,b], N. Oijeabou [a], C. Koerner [a], Y. Michael [a],
B. Oloruntoba [c], C. Montzka [c], H. Vereecken [c], H. Hendricks Franssen [c], J. Brendt [f], S. Brauner [a],
W. Kuckshinrichs [e], S. Venghaus [a,g], D. Kone [g], B. Korgo [h,k], K. Ogunjobi [h], V. Chiteculo [i],
J. Olwoch [i], Z. Getenga [j], J. Linßen [a], D. Stolten [a,b]

[a] *Forschungszentrum Jülich GmbH, Institute of Energy and Climate Research – Jülich Systems Analysis (IEK-3), 52425 Jülich, Germany*
[b] *RWTH Aachen University, Chair for Fuel Cells, Faculty of Mechanical Engineering, 52062 Aachen, Germany*
[c] *Institute of Bio- and Geosciences: Agrosphere (IBG-3), Forschungszentrum Jülich GmbH, 52425 Jülich, Germany*
[d] *Center for Remote Sensing and GIS Research, Faculty of Earth Sciences, Shahid Beheshti University, Tehran, Iran*
[e] *Forschungszentrum Jülich GmbH, Institute of Energy and Climate Research – System Analysis and Technology Evaluation (IEK-STE), 52425 Jülich, Germany*
[f] *Forschungszentrum Jülich GmbH, Corporate Development, (UE), 52425 Jülich, Germany*
[g] *RWTH Aachen University, School of Business and Economics, 52062 Aachen, Germany*
[h] *West African Science Service Centre on Climate Change and Adapted Land Use (WASCAL), Agostino Road, PMB CT 504, Accra, Ghana*
[i] *Southern African Science Service Centre for Climate Change and Adaptive Land Management (SASSCAL), 28 Robert Mugabe Avenue, Windhoek, Namibia*
[j] *Machakos University, Machakos County, Kenya*
[k] *University Joseph KI-ZERBO, Ouagadougou, Burkina Faso*

ARTICLE INFO

ABSTRACT

For fast-tracking climate change response, green hydrogen is key for achieving greenhouse gas neutral energy systems. Especially Sub-Saharan Africa can benefit from it enabling an increased access to clean energy through utilizing its beneficial conditions for renewable energies. However, developing green hydrogen strategies for Sub-Saharan Africa requires highly detailed and consistent information ranging from technical, environmental, economic, and social dimensions, which is currently lacking in literature. Therefore, this paper provides a comprehensive novel approach embedding the required range of disciplines to analyze green hydrogen cost-potentials in Sub-Saharan Africa. This approach stretches from a dedicated land eligibility based on local preferences, a location specific renewable energy simulation, locally derived sustainable groundwater limitations under climate change, an optimization of local hydrogen energy systems, and a socio-economic indicator-based impact analysis. The capability of the approach is shown for case study regions in Sub-Saharan Africa highlighting the need for a unified, interdisciplinary approach.

1. Introduction

In the wake of the rising cases of extreme weather conditions around the globe and the huge socio-economic losses and impacts driven by climate change, interventions relying on the use of green hydrogen as a decarbonization energy carrier has become a popular topic. At regional but also national and international levels, strategies to guide the production and use of hydrogen have been widely reported [1,2]. China for example has launched a hydrogen strategy targeting the transportation

sector with measures to promote fuel cell vehicles [2]. The EU hydrogen strategy, which was adopted in 2022 prioritizes green hydrogen, and is committed to building a 40 GW electrolyzer capacity by 2030 [3]. It has the following five policy focuses: investment support, support production and demand, creating a hydrogen market and infrastructure, research and development, and international cooperation. The National Clean Hydrogen Strategy and Roadmap of the United States of America [4] published in 2023 lays out pathways of leveraging clean hydrogen for the decarbonization of the various sectors of the economy. It plans to

produce 10, 20 and 50 million metric tons of clean hydrogen annually by 2030, 2040 and 2050 respectively, resulting in a 10% reduction in greenhouse gas emissions [4]. The German National Hydrogen Strategy was renewed in 2023 by the Federal Ministry for Economic Affairs and Climate Action [5] detailing steps to accelerate the rollout of technology for the sustainable production and utilization of hydrogen. For its domestic industries, up to 130 TWh of hydrogen will be required by 2030 for which a 10 GW generation capacity for green hydrogen must be established. In total, 50–70% of the hydrogen demand is expected to be imported from European and international sources in the form of green hydrogen.

In Africa, green hydrogen strategies are on the rise as well. The Economic Community of West African states, ECOWAS launched her regional green hydrogen policy and strategy framework which has been adopted by the member states. It lays out that green hydrogen will play a key role for the subregion in aiding transition to green economy as well as mitigating climate change. It sets a short-term target of producing 0.5 million tons of green hydrogen annually by 2030 and a long-term target of 10 million tons by 2050 [6]. Kenya launched her green hydrogen strategy in 2023 with the ambition to install 100 MW electrolysis capacity by 2027 and potential to scale up to 250 MW by 2032. The focus is for local green fertilizer production and for export [7]. All of these strategies combined with the huge renewable energy resources is to provide a workable framework for the implementation of hydrogen projects in Africa. Beyond these, the ECOWAS strategy for example makes it clear that there is the need for win-win partnerships to support the development of green hydrogen in Africa. These partnerships must recognize and consider local contexts through stakeholders' engagement in technology deployment and capacity building in order to guarantee local value and support. In Southern Africa, South Africa has been in the forefront of hydrogen development with the launch of its hydrogen research, development and innovation strategy, the so-called Hydrogen South Africa, HySA in 2008 [8]. HySA aims to position South Africa to actively drive hydrogen and fuel cell production and utilization along the entire value chain. HySA seeks to harness South Africa's mineral deposits and promote its cost-effective and sustainable use in the hydrogen economy and renewable energy. The Hydrogen Society Roadmap for South Africa 2021 builds further on HySA with a 70 action points to further boost the development of hydrogen in South Africa [9]. The actions focus on hydrogen production, storage and distribution, decarbonization of transport, creation of export market among others [9]. Namibia is another country in Southern Africa making giant strides in advancing green hydrogen technology. In its strategy document released in 2022, Namibia hopes to generate up to 12 million tons of hydrogen annually by 2050 from its three hydrogen valleys: southern region of Kharas, the central region including Walvis Bay port and the capital Windhoek, and the northern region of Kunene [10].

Sub-Saharan Africa is a very promising region for green hydrogen production given its huge renewable energy resources. Africa has over 31 PWh/a renewable energy capacity [11] that has mainly remained untapped. This huge potential can play a key role in drastically increasing local energy access. Beyond a part of this can be harnessed and utilized for green hydrogen production to balance variable renewable energy feed-in and for export. This way, the region has a clear path towards a 100% green energy access but also for economic opportunities arising from a green hydrogen economy.

In each of the touched research areas, several works have been done, even if not jointly, across the decisive dimensions for a green hydrogen economy in Sub-Saharan Africa. Starting with studies assessing renewable energy potential in that region, a lot of work has been done to quantify the available renewable energy resources in Africa in general. Winkler et al. [12] implemented the so-called Integrated Renewable Energy Potential Assessment for assessing smallholder farming systems in South Africa. The authors opined that consideration should be given to the various inter-related social, environmental and technological factors to properly estimate RE potential. Spatially explicit models and long-term satellite data have also been used to assess offshore wind technical potentials (Elsner, 2019). Especially for the African continent, Mentis et al. [11] estimate that an annual potential from onshore wind generation could reach up to 31 PWh based on the technical potential, but only calculates timeseries daily. Within a global assessment, Bosch et al. [13] determine annual time series for Africa, combining simulation methods from weather data with a suitability approach for potential estimation. For PV, global studies for technical potentials exist as well like Pietzcker et al. [14] and Köberle et al. [15]. For the ECOWAS region, Yushchenko et al. [16] analyzed the potentials for open field PV using a multi-criteria decision analysis combining technical potential evaluation with feasibility factors like distances to grid connections or roads and therefore not limiting the potentials to a technical feasibility.

The body of literature on green hydrogen potential, however, predominantly focuses on European nations, as evidenced by several peer-reviewed studies [17–19]. However, there is a noticeable paucity of research addressing low-income countries, particularly within the sub-Saharan African region (Müller, 8). Despite this, the International Renewable Energy Agency [20] has estimated that Sub-Saharan Africa possesses the greatest potential to produce green hydrogen for under 1.5 USD/kg by 2050, with 30 times more potential than all of Europe [21, 22].

Unfortunately, comprehensive studies evaluating the potential for hydrogen production in Sub-Saharan African countries remain lacking. For instance, while Asare-Addo et al. [23] have examined the potential of generating green hydrogen from wind and solar energy in Ghana, their land suitability assessment lacks various relevant criteria and doesn't incorporate detailed placements of solar parks or wind turbines. Similarly, Bhandari et al. [24] analyzed the production of hydrogen from solar resources to meet the projected hydrogen demand in 2040 for Niger, utilizing assumed land area sizes for various land categories based on literature values. This approach may not reflect the latest changes in land use, as land-use datasets are continuously updated.

Müller et al.'s [25] simulation-based approach for evaluating the potential cost of hydrogen in high resolution identifies the most cost-effective locations for potential green hydrogen production and to meet a specified demand, as demonstrated in Kenya. However, the methodology employed in their approach relies on average power potential data from presumed photovoltaic (PV) and wind turbines to calculate annual generation value. This approach may not yield the most precise estimate, as the generation from wind and PV sources can exhibit significant fluctuations over time. Ayodele & Munda [26] use real hourly wind speed data measured at a height of 60 m to assess the site-specific cost of hydrogen production. Their study focuses on the impact of the operating characteristics of 11 different wind turbines on hydrogen production at 15 sites across five major provinces in South Africa. However, the study does not evaluate the overall potential of hydrogen production from wind turbines across South Africa.

Gado et al. [27] evaluated the potential for hydrogen production by 2030 from solar and wind resources at a county level for African nations. The study considered water scarcity and other obstacles in the analysis, but there are a few limitations. The study did not take into account land-use restrictions, and therefore did not model the placement of solar or wind parks. Additionally, the model did not incorporate the co-optimization of solar and wind resources and thus overlooked the complementarity effect of solar and wind generation.

Franzmann et al. [28] conducted a comprehensive analysis of cost-potential curves up to 2050 for 28 specific countries globally including Namibia. The study primarily focuses on assessing how the complete green hydrogen process chain design impacts hydrogen production costs for export purposes only. Nevertheless, the research involved a detailed assessment of land eligibility based on 38 different criteria and modeling the placement of open-field PV and onshore wind turbine sites. Subsequently, these sites were simulated to generate hourly energy output time series using MERRA-2 weather data.

In addition to hydrogen potentials, Mukelabai et al. [29] show, that

for producing green hydrogen from renewables, water limitations in Sub-Saharan-Africa play a crucial role for electrolysis. Therefore, it is essential to take particular care to ensure the sustainability of water supply for green hydrogen production. Considering that for producing 1 kg of hydrogen, a consumption of 9 kg of water is required [30], a substantial supply of water resources is required. Especially in regions, which already face substantial water security challenges, like those in Sub-Saharan Africa [31]. In this context, groundwater has gained widespread recognition as the primary water source sustaining diverse communities across the African continent [32].This acknowledgement is based on its ubiquitous presence, consistent availability, substantial storage capacity, superior water quality, and resilience to variations in both annual and seasonal climates, setting it apart from other available options [33–36]. Additionally, according to the United Nations Environment Programme (UNEP) in 2010, the large groundwater storage capacity solidifies its status as the most abundant water resource in Africa [37]. These characteristics make groundwater an attractive and essential source for sustainable new energy production in Africa. A thorough assessment of groundwater availability in Africa is considered not only to foster beneficial hydrogen production, but also to implement sustainable water consumption strategies to prevent the over-exploitation and depletion of groundwater reserves [38–41], and avoid potential conflicts among diverse water users. To unlock the option for green hydrogen production in regions without sustainable groundwater the option to supply water through seawater desalination has gained much attention as well [28].

To ensure a sustainable water supply, our attention is directed towards the sustainable yield of groundwater. This refers to the amount of groundwater available for extraction that can be utilized over an extended period without causing negative effects, while also maximizing economic, social, and environmental benefits [42–49]. To quantify the groundwater sustainable yield, it is essential to consider groundwater recharge in addition to total human (sectoral) water usage and environmental flow. Groundwater recharge plays a vital role in assessing groundwater sustainability and forecasting future changes [50,51]. It can be derived either locally from nearby water bodies or in a more diffuse manner from precipitation over unsaturated soil zones. Over the long term, diffuse recharge represents the portion of precipitation that does not evaporate or contribute to surface runoff and interflow into surface water bodies [35]. This study specifically examines diffuse recharge, and therefore, "groundwater recharge" will primarily refer to this type. Estimating groundwater recharge in both spatial and temporal dimensions is challenging due to the lack of a universally applicable method to directly measure the amount of rainfall reaching the groundwater table [52,53]. Nonetheless, several indirect methods are available for estimating groundwater recharge at various scales. The most commonly employed techniques include chloride mass balance, environmental and isotopic tracers, groundwater-level fluctuation methods, and the estimation of baseflow to rivers through hydrological models [54]. On a global scale, the initial groundwater recharge study was conducted in 1979 by L'vovič [55]. This study utilized a baseflow component of measured river discharge to create a comprehensive global map of groundwater recharge Ĺvovich, 1979. Subsequently, global groundwater recharge has primarily been estimated through the utilization of hydrological models. For instance, Döll et al. [56] generated a global groundwater recharge map by means of the hydrological model WGHM (WaterGAP Global Hydrology Model [57, 58]), and updated simulations with the WGHM2 model [35]. Considerable research efforts have been dedicated to investigating various facets of groundwater recharge across numerous regions in Africa, for instance, in southern Africa [59,60], northern Africa [61–63] and western Africa [64–67]. The first comprehensive long-term groundwater recharge map covering the entirety of Africa was produced, spanning from 1970 to 2019. This map was created using estimates gathered from ground-based measurements [54]. Utilizing hydrological and land surface process modeling to estimate groundwater recharge allows for the

incorporation of soil and vegetation effects on recharge. Earlier research has emphasized the important role of land cover and soil types in influencing the relationship between precipitation and groundwater recharge [68–70]. Characteristics of land cover, such as vegetation density and the presence of impervious surfaces, significantly affect water movement and infiltration processes. Vegetation facilitates groundwater recharge by enhancing infiltration, whereas impervious surfaces obstruct infiltration and lead to increased surface runoff [71]. More recently, five decades (1965–2014) of groundwater recharge simulations have been performed by means of CLM land surface process model for African continent to investigate groundwater sustainability and encourage its sustainable consumption [72].

Regarding the socioeconomic dimension renewable energy (RE) holds the potential for positive impacts [73], influencing areas such as job creation, local economic development, energy security, and social equity. To accurately measure and assess these impacts, it is imperative to employ suitable indicators. Composite indicators (CIs) provide a valuable means of aggregating the numerous individual factors inherent in each case, thereby enhancing measurability and analyzability [74]. Recent research indicates a continual expansion and refinement in the application of composite indicators. The development of these indicators has been instrumental in capturing the complex, multidimensional impacts of renewable energy on both macro and microeconomic scales. For instance, a study by Borbonus [75] introduces a framework that dissects the potential social and economic benefits of renewables into subcategories that can be adapted to the specific needs of each country. Another framework presents a scalable and internationally transferable methodology for a composite index of the risk of energy poverty in domestic heating [76]. This developed CI by Kelly et al. [76] is particularly relevant in the context of policies aimed at ensuring a just transition to sustainable energy systems.

Further examples of the utility of CIs in addressing complex issues such as renewable energy include a study identifying connections between access to electricity and social development [77]. The relationship between electrification and social development is a key area of study, with research suggesting that access to electricity not only drives economic growth but also improves quality of life, particularly in developing regions. The authors conclude, based on their indicator analysis, that "electrification of social infrastructure can serve as an energy anchor, facilitating and enlarging electrification of neighborhood communities and productive use [78]". Research assessing an energy poverty index indicates that the broader implementation of sustainable energy sources can contribute to alleviating energy poverty [79]. Similar findings were also uncovered in a CI-based study examining the impact of RE production at specific levels of urbanization [80]. Additionally, more recent studies have focused on the socioeconomic benefits of decentralized renewable energy systems, particularly in rural and underserved communities. For example, Alstone et al. [81] discuss how off-grid solar projects can lead to job creation, improved health outcomes, and enhanced educational opportunities in remote areas. Moreover, the work by Mazzucato and Semieniuk [82] highlights the importance of public investment in driving the deployment of renewable energy technologies and ensuring that their socioeconomic benefits are widely shared. These studies collectively emphasize the need for a multidimensional approach in evaluating the impacts of renewable energy, considering not only economic factors but also social and environmental dimensions.

Recognizing the relevance of renewable energy resources in green hydrogen production and understanding the potential scale of such production is pivotal in addressing the political and socio-cultural challenges associated with integrating hydrogen into the national energy mix of Sub-Saharan African countries. This study proposes a novel, interdisciplinary methodology that incorporates the participation and preferences of local stakeholders to elucidate the green hydrogen potentials in selected parts of sub-Saharan Africa. Such an approach necessitates a comprehensive assessment of renewable energy resources,

taking into account the local contexts and preferences derived from extensive socio-economic, techno-economic, ecological, and local stakeholder engagement. The unique land use and tenure system in Africa underscores the importance of a well-articulated land eligibility assessment (LEA) for hydrogen production, conducted in collaboration with local stakeholders.

This research presents an in-depth analysis of the potential for green hydrogen production, with a particular focus on countries in Sub-Saharan Africa. The aim is to provide a detailed account of the methodology employed to determine the total green hydrogen production potential and the associated unit cost, as demonstrated in selected regions within Sub-Saharan Africa. To the best of our knowledge, at the time of writing, no other study has comprehensively considered the integration of technological, environmental, and local contextual factors, incorporating both theoretical, analytical, experimental, and social approaches. This holistic approach is unique and has not been thoroughly explored in previous studies. The methodology is presented in Section 2, and the findings are detailed in Section 3. Section 4 offers a critical reflection on the applied approach and the resultant findings.

2. Methodology

The underlying methodology of this study consists of several coupled models and integrated data to finally achieve its given goal to serve as decision support shown. The chosen methodology has been already employed in several publications ([12,83,84] Ishmam et al., 2024) and refinements considering preferences of local partners in Africa were included. To illustrate the methodology here a exemplarily region in Sub-Saharan Africa is used. It starts with a dedicated land eligibility analysis which identifies where renewable energy technologies can be placed in accordance with local preferences. Based on those placements each location specific wind turbine and open-field photovoltaic module are simulated to derive their weather dependent hourly electricity generation. In parallel, the availability of sustainable groundwater and the cost for seawater desalination are calculated mostly based on [72]. In a next step, both water supply options together with the time series of renewable energy technologies are fed into an energy system model for each "GID-2" administrative region based on the definition from Global Administrative Areas [85] in the analyzed regions. Each energy system model additionally consists of batteries as potential electricity storage, hydropower plants and electrolysis to supply an exogenously increasing hydrogen demand until the maximum potential is achieved to form a green hydrogen cost-potential curve for each region. In addition to these techno-economic results, the methodology was extended by drawing on previous studies that overlooked aspects related primarily to socio-technical and socio-economic factors. Indeed, since energy projects would provide local added value and could be beneficial in those regions, where the energy supply is not yet fully developed, opportunities for the population should be explored. Together these results are made available via a web-based graphical user interface (GUI) to be accessible for a wide range of decision-makers and stakeholders.

2.1. Land eligibility assessment for open-field photovoltaic and onshore wind turbines

A land eligibility analysis that yields the overall land area eligible for the placement of renewable plants under specified constraints usually comes before determining the theoretical maximum renewable potential like for onshore wind [86–88]. Typically, the land eligibility analysis takes into account various factors such as topography, land use, environmental constraints, and social and economic considerations [89]. Within the context of this study, the set of land eligibility criteria have been carefully selected from literature sources [28,89] and complemented by feedback received from our local partners. As this study focuses specifically on Sub-Saharan Africa, the inclinations of regional stakeholders, such as community members, governmental bodies, and

international institutions are of utmost importance to achieve meaningful results for decision makers. Therefore, deliberate efforts have been made to collect, process, and examine the local preferences aligned with the criteria listed in Table 1 within several workshops. The set of constraints thus obtained are referred to as "local preferences" in the subsequent sections. In cases where it was not possible to receive stakeholder preferences, the median of the local preferences collected was allocated. This has been done for onshore wind turbines and open-field photovoltaics, which are perceived as major building blocks of the global energy transition with comparable low environmental impact [90]. This approach results in 33 criteria and buffer distances for onshore wind and open-field PV each.

The research was conducted using the open-source general-purpose geospatial toolkit GeoKit [91] and the land eligibility model "Geospatial Land Availability for Energy Systems" (GLAES) [92]. GLAES leverages the capabilities of GeoKit to perform all its underlying geospatial operations and is specifically designed for land eligibility analysis. Its design focuses on reducing errors that may arise from geospatial operations commonly needed for land eligibility analysis, being transparent in methodology, scalable for vast geographical regions, and adaptable to standard geospatial data formats. Both GeoKit and GLAES are implemented in the Python 3 programming language and rely on the SciPy [93] ecosystem for general numerical and matrix computations and the Geospatial Data Abstraction Library (GDAL) [94] for geospatial operations, both of which are open-source projects. The computations for the land eligibility analysis were conducted using a custom Lambert azimuthal equal-area projection (LAEA) projection system with a 100 m spatial resolution centered on each region individually, which provide the highest accuracy for the area determination. The exclusion features are the most comprehensive in comparable studies to date. In combination with carefully selected high-resolution geospatial datasets that are particularly suitable for the project region, the resulting land eligibility has an unprecedented degree of reliability. This allows geospatial exclusions even against high resolution satellite imagery. However, it is not able to capture exclusions that are not clearly defined by geospatial properties, such as the objection of landowners or lawsuits due to, for example endangered species that are found in the area only upon local inspection.

Fig. 1 displays an exemplary case of how land exclusions correspond to each criterion in a region in Sub-Saharan Africa. The application of each criterion, with its associated buffers, such as 200 m around primary roadways, 1000 m around settlements, etc., results in the progressive exclusion of more and more land areas. As a result, only a mere 23.8% of the land area is available for this exemplary region.

Based on the collected local preferences, land exclusions were applied for all 33 criteria and eligible areas were computed for each

Table 1
Selected criteria for land eligibility analysis.

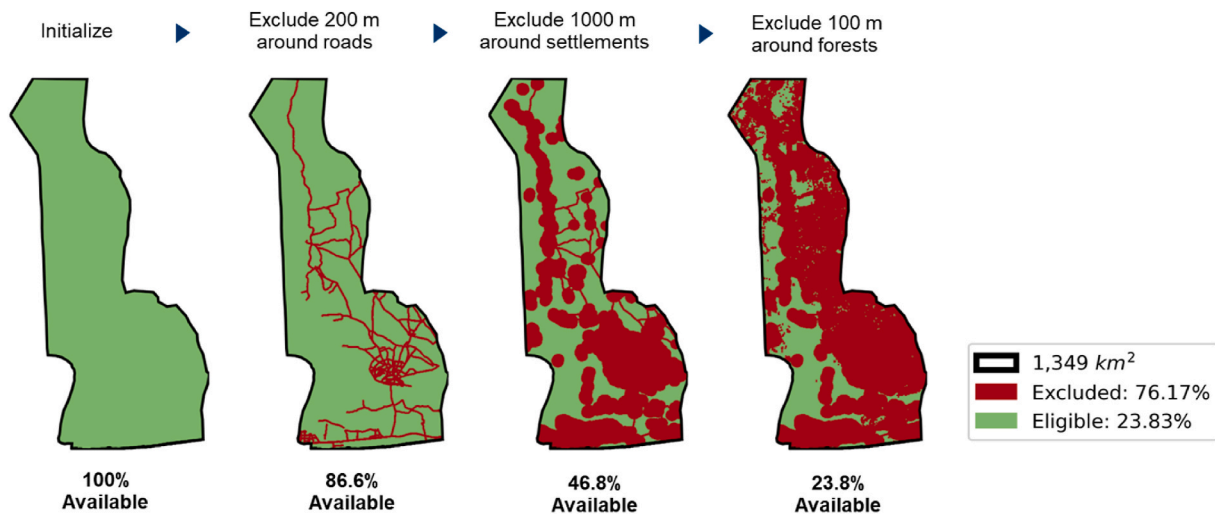| Criteria			
1	Settlements (connected)	18	Lakes
2	Settlements (isolated)	19	Creeks
3	Airports	20	Rivers
4	Primary Roadways	21	Coastlines (Ocean, general)
5	Secondary Roadways	22	Woodlands (All Forests)
6	Agricultural Areas	23	(Standard) Wetlands
7	Pasture Areas	24	Specially protected Wetlands
8	Railways	25	Sand Dunes
9	Power Lines	26	Natural Habitats
10	Historical Sites	27	Biospheres
11	Recreational Areas	28	Wildernesses
12	Leisure and Camping	29	Bird Areas
13	Industrial Areas	30	Protected Landscapes
14	Commercial Areas	31	Natural Reserves
15	Mining Sites	32	National Parks, State Parks, etc.
16	Military Areas	33	Natural Monuments
17	National Borders		

Fig. 1. Exemplary exclusion of different criteria for an example region in western Africa (Ouémé in Benin)
* The buffer distances used here are solely for illustrative purposes.

region for both wind turbines and photovoltaic modules. A meticulously curated compilation of the primary open-source geospatial datasets utilized for implementing the exclusions corresponding to the 33 selected criteria is accessible online via the GUI (https://africa.h2atlas.de/). The selection of these datasets is based on the methodology applied by Franzmann et al. [28] and Ryberg et al. [89].

The resulting eligible areas form the basis for the renewable energy potential assessment in Section 2.2.

2.2. Renewable energy potential assessment

Subsequently, wind turbines and open-field PV modules are placed on eligible areas. For this wind turbines are positioned with a distance of 8 times the rotor diameter for the main wind speed direction and 4 times the rotor diameter for the transversal wind speed direction using the placement algorithm in GLAES [95]. The turbines utilized here are specifically designed for future applications and are extensively examined in Ryberg et al. [95], as the applied scenario is specifically framed for the year 2050. Hourly simulations are then conducted using the appropriate meteorological data from the ERA-5 weather data source [96] for the corresponding year, following the methods outlined in Ryberg et al. based on the open-source tool RESKit [95,97]. The RESKit [97] toolkit not only facilitates high spatiotemporally resolved simulations of solar and wind resources but also allows evaluating the investment cost of each individual solar and wind placement through the utilization of a cost model.

Similarly, simulation sites for open-field PV parks are placed with a minimum distance of 1000 m between them. When considering PV parks, the area surrounding each placement is an important factor in its potential capacity, as they are much more spread out than wind parks. Eligible area in the case of PV parks is assigned by creating Voronoi polygons [98] at a size of 1000 m around each possible placement location and grouping adjacent and non-contiguous eligible area together. As a last step, the placement locations are updated to correspond to the centroid of each identified area. For this technical potential an open-field coverage of 20 m^2/kW$_p$ and the module Winaico WSx-240P6, as suggested by Ryberg [84] is assumed. Finally, all the locations are simulated for open-field PV systems without single-axis tracking, using the algorithm of RESKit described in Ref. [84]. We selected a fixed PV system as it has the lowest investment cost, which is especially relevant for countries potentially facing financing challenges.

The ERA-5 reanalysis dataset has been chosen since several recent studies have evaluated ERA-5 as significantly better for modeling wind and solar resources than other reanalysis datasets such as MERRA-2 [99,

100]. Using climate model output datasets such as ERA-5 is the most practical solution due to the large spatial domain, the need for various weather parameters, and the requirement to assess wind generation over multiple years to accurately represent the wide range of potential weather events. Our thorough evaluation process, which takes into account the uncertainties and potential biases associated with using climate model outputs, reassures the validity of our results [101–104].

The hydropower potentials in Africa from Sterl et al. [105] were utilized to derive the electricity generation time-series available from existing and planned hydropower plants in Africa. The database offers monthly hydropower generation data under three distinct scenarios: "dry," "normal," and "wet" seasons. For this analysis, the "normal" scenario was adopted as it represents a standard performance of the hydropower hydro-fleet according to the author. In addition, its use allows for hydropower production estimation potential under no extreme conditions. Only hydropower plants with a capacity exceeding 1 MW were included in the analysis, encompassing both run-of-river and reservoir hydropower facilities. This makes 394 medium and large hydropower plants total with 84 GW installed capacity for 2050 considered in the assessment. To align with the temporal resolution of wind turbines and PV modules, the monthly generation time series was transformed into an hourly form by linearly projecting the monthly generation into hourly values from one month to the next. The monthly mean values were assigned in the middle of the month. Hydropower costs were taken from the report "Renewable Power Generation Costs in 2019" from IRENA [106].

The geothermal potentials are based on a methodology from Franzmann et al. [107]. Based on the land eligibility results from section 2.1 for geothermal plants, the capacity for enhanced geothermal systems is calculated. The geological temperature is estimated based on an approach from Aghahosseini et al. [108] and heat flow data from Goutorbe et al. [109]. The heat output of the plants is calculated based on Gringartens approach [110,111] applied to location specific plants and the thermal conversion is based on Tester [112]. As geothermal cost is mostly dependent on drilling costs, the medium outlook of geothermal drilling costs is assumed based on NREL [113] for a maximum depth of 7 km [112].

The resulting time series of electricity generation of each wind turbine, open-field PV park and hydropower plants form the supply basis for the subsequent step to derive the green hydrogen potential.

2.3. Sustainable water supply assessment

For the assessment of water availability, we considered sustainable

groundwater supply and seawater desalination including water transport. The long-term groundwater sustainable yield has been estimated by integrating detailed land surface hydrology and natural groundwater recharge simulations at 10 km spatial resolution. This analysis was conducted using the Community Land Model [version 5] (CLM) [114] and supplemented with data on sectoral water usage [115] across Africa. This model-based approach is particularly valuable as it captures spatio-temporal variations, including atmospheric forcings, land cover, and soil texture, thereby providing comprehensive insights into land surface hydrology, such as evapotranspiration and surface runoff. By considering sustainable groundwater supply and and seawater desalination options, all regions have a potential source of water supply.

2.3.1. Sustainable groundwater supply

2.3.1.1. Groundwater recharge.
The annual groundwater recharge was determined through simulations using the CLM5 model [114] employing a widely-used water balance method [72,116–118]. Furthermore, to account for anthropogenic water inputs, the water balance integrated irrigation, following CLM simulations [119], as indicated by:

$$R = (P + I) - ET - Q \tag{1}$$

where R is groundwater recharge [mm yr^{-1}], P is the precipitation (rain and snow) [mm yr^{-1}], I is the simulated irrigation by CLM5 to account for all anthropocentric water supply [mm yr^{-1}], ET is evapotranspiration [mm yr^{-1}], and Q is surface runoff [mm yr^{-1}]. Groundwater recharge was estimated on a yearly basis.

2.3.1.2. Environmental flow.
Environmental flow (Qrest), or the minimum ecological water requirement, represents the essential water volume crucial for sustaining ecosystems and the services they provide. Previous recommendations advocate that the responsible use of water resources should not exceed 10%, 40%, and 70% of the total groundwater recharge, aligning with conservative, medium, and extreme scenarios [47,48,120,121]. In accordance with these guidelines, we have adopted three distinct scenarios to allocate environmental flow based on the simulated groundwater recharge: (i) a conservative scenario (90% of recharge), (ii) a medium scenario (60% of recharge), and (iii) an extreme scenario (less conservative with 30% of recharge).

2.3.1.3. Sustainability analysis.
Determining the groundwater sustainable yield involves the application of Eq. (2), which incorporates the concept of the percentage of recharge, as suggested by Ref. [116,122], alongside the integration of total sectoral water consumption. This method enables the assessment of the sustainability of groundwater utilization.

$$SY = R - Qrest - SWU \tag{2}$$

where SY is groundwater sustainable yield, Q_{rest} is environmental flow, and SWU is sectoral water use. The units of all variables in Eq. (2) can be expressed in mm yr^{-1}.

Moreover, we have considered three distinct scenarios for the sustainable yield derived from the three environmental flow scenarios (conservative, medium, and extreme). For groundwater availability analysis, the long-term (2015–2100) groundwater sustainable yield has been calculated, and then the average from 2015 to 2035, 2015–2045 and 2036–2065 are considered representative of 2020, 2030 and 2050. The groundwater recharge is obtained from the CLM5 model [114] simulations at 10 km spatial resolution, forced by the regional climate model runs of CCLM5 [123], REGCM4 [124], and REMO2015 [125], which were driven by the MPI [126] and NOR-ESM [127] General Circulation Models (GCMs). Such regional climate models and GCM simulations from the CORDEX dataset (https://cordex.org/; last accessed: November 1, 2023) are utilized due to their extensive long-term spatial coverage over the targeted regions in Africa. The RCP2.6 (which is

considered optimistic indicating low greenhouse gas concentration pathways) and RCP8.5 (which is considered pessimistic indicating high greenhouse gas concentration pathways) scenarios were considered for these simulations. The average groundwater recharge (from six combinations of GCMs and RCMs), and consequently the groundwater sustainable yield, is considered for further use in the green hydrogen project for RCP2.6 (optimistic) and RCP8.5 (pessimistic) scenarios. The environmental flow is calculated from simulated groundwater recharge. The sectoral water use is obtained from literature [115] that takes total water withdrawal for industrial, irrigation, domestic, and livestock into account.

2.3.2. Desalinating seawater and water transport
The selection of groundwater or desalinated water for hydrogen production depends on the cost incurred. Since groundwater is usually the cheaper option, this means that local groundwater resources are considered first, and desalinated seawater is used once the limits of sustainable groundwater are reached. Regions that do not have sustainable groundwater resources left have to use exclusively desalinated water. After a comparison of published literature on water transport cost, a validated UN cost model [128] based on real data [76] was selected to integrate water supply from seawater desalination in our analysis. This updated model requires the electricity cost for pumping as well as elevation and distance to the shore as an input. This base model was further developed by updating cost values and converting diesel-to-electricity-powered pumps. Electricity cost was introduced as a variable and set to the average solar photovoltaic levelized cost for 24-h operation: Exemplary studies in the affected regions revealed that, under the given techno-economic assumptions, the unit cost for constant operation amounts on average to ca. 3x the solar electricity production cost due to the required extra cost for battery storage. Transport distance is then calculated based on distance of the district centroid from the nearest coastline [129] and a detour factor of 1.3 typical for infrastructure routing [130]. Elevation is extracted as the average regional value from OpenTopography [131]. Desalinated water cost is calculated using the cost model of Loutatidou et al. [132], scaled to present day cost, with the previously mentioned PV-based electricity cost and a reference plant size of 367 000 m^3/h, based on Heinrichs et al. [133].

2.4. Local green hydrogen potential assessment

In this study the technical hydrogen potential for each "GID_2″ region has been evaluated. The "GID_2″ regions refer to the administrative divisions of the second level as categorized by the GADM (Database of Global Administrative Areas) [85]. In countries where no "GID_2" level is available, the first level "GID_1" divisions were used. In the following analysis, the simplified term "GID_2 regions" will be used for all regions for improved readability. For each of these GID-2 regions a separate energy system model was defined containing the components shown in Fig. 2.

To determine the maximum amount of hydrogen that may be produced in each GID_2 region and to calculate the related levelized cost of hydrogen (LCOH), an independent energy system model was created for each region and optimized using the ETHOS.FINE (Framework for Integrated Energy System Assessment) optimization framework within the ETHOS model suite. The optimization framework was previously described by Welder et al. [134] and Groß et al. [135] and a publicly accessible version of the framework can be obtained from Github (FINE, 2024).

In the developed ETHOS.FINE model, each region is represented as one node, and an energy system is optimized for each node with several components. Onshore wind turbines, open-field PV parks, and existing hydropower plants were utilized as electricity sources, PEM electrolysis as green hydrogen production technology, and Li-ion batteries for electricity storage. Their assumed techno-economic parameters required for the optimization are listed in Table 2. For all these components the
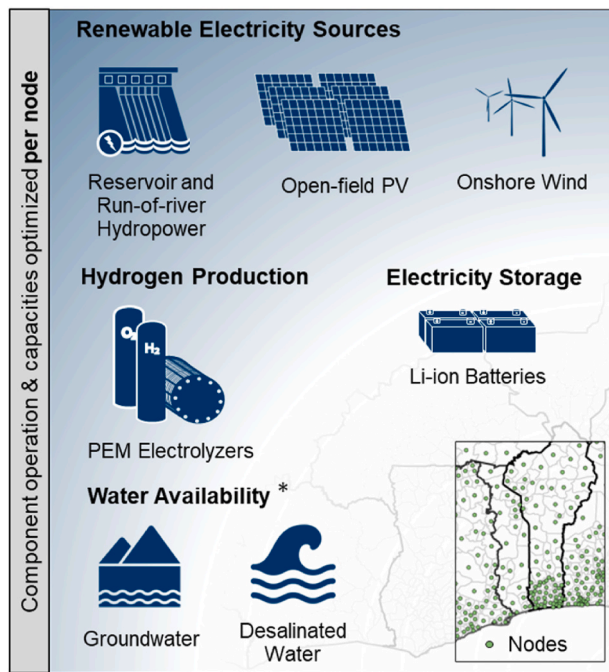
Fig. 2. Set of components added to each node of the model. * *Icons made by Ayub Irawan and orvipixel from* www.flaticon.com.

optimal capacity and operation in hourly resolution is optimized, while fulfilling an exogenously assumed gaseous hydrogen demand. The exogenous demand for hydrogen at each node incrementally raised in increments of 6% on average until the node's maximum hydrogen production capacity was depleted. The linear optimization minimized the annual cost of the necessary hydrogen production system and determining the most cost-effective technology portfolio for each node.

The renewable energy potential for onshore wind, open-field PV and the existing and planned hydropower capacities were aggregated from individual plant-level time-series to LCOE clusters per each GID_2 region. The LCOE range for wind turbines and PV within each GID_2 region was therefore split into 10 evenly spaced bins for each technology and the capacity-weighted average time series was calculated for each bin. In case of wind, the number of regional LCOE clusters was doubled to account for the high variation of wind potentials within even small geographical extent. As hydropower relies on few locations with possibly very different characteristics, especially when not depending on the same catchment area, the hydropower locations were not further clustered.

The projected local electricity and hydrogen demand should be prioritized over export countries to ensure local living standards and development as well as the acceptance of potential export schemes beyond local demand [137]. Therefore, local electricity and hydrogen demand is deducted from national hydrogen potentials in a subsequent step.

2.5. Socio-economic impact assessment

This study's research approach was developed using the OECD checklist for the reflective construction of composite indicators [138], a widely recognized framework for ensuring robustness and transparency in indicator selection. The decision to use this method was based on its ability to systematically address multidimensional phenomena, such as sustainable development, by providing a structured process for indicator selection, weighting, and aggregation. The OECD approach was particularly suited to this study as it aligns with the complex and interconnected nature of the Sustainable Development Goals (SDGs), which require careful consideration of both direct and indirect effects. Its main components are summarized in Table 3.

Data sets were selected with a focus on sustainable development, prioritizing indicators that capture the most significant impacts of green hydrogen projects. This selection process was guided by the need to identify SDGs that are either directly or indirectly influenced by green hydrogen initiatives. Firstly, the more direct impact would be on Goal 7 (affordable and clean energy) and Goal 8 (decent work and economic growth), as an increase in hydrogen projects leads to a concurrent increase in renewable energy capacity. Secondly, green hydrogen projects could indirectly affect goals 1 (no poverty), 2 (zero hunger), 3 (good health and well-being), and 13 (climate action). Economic growth and employment, ideally, could contribute to poverty reduction, enabling more individuals to afford food and healthcare. Additionally, the increase in green energy and clean fuel would have a positive impact on areas affected by indoor pollution and hazardous fossil fuel emissions, aligning with the imperative for climate action.

Further research, complemented by spatial data analysis, was conducted to assess the feasibility of socio-economic indicators in measuring the defined SDGs. This analysis was essential for ensuring that the selected indicators could be desegregated at the regional level. Additionally, ant to accurately reflect the local context to effectively guide policy-making, the study also incorporated the prioritization of social development goals based on local visions, as revealed in surveys conducted during the project [137].

Table 3
Employed socio-economic composite indicators.

Sub-category	Indicator	Components	Unit
Access to Energy	Access to electricity	Population without access to electricity per GID_2 region's area	Capita/km^2
Macroeconomic effects	Direct employment factor	Labour employment potential per installed capacity and per GID_2 region's area	Jobs/ (Mwp*km^2)
Other indirect effects	Dependence on traditional biomass	Population using traditional biomass per GID_2 region's area	Capita/km^2
	Population living under the poverty line	Share of the population under the poverty line	%

Table 2
Techno-economic assumption parameters for each component [106,136]

Parameter	Investment [€/kW] respectively [€/kWh]				Fix O&M [% of CAPEX]	Variable O&M [€/kWh]	Economic Lifetime
Year	2020	2030	2040	2050	2020–2050	2020–2050	2020–2050
Onshore Wind[a]	1290	1130	1050	1000	2.5	–	20
Open-field PV**	690	450	370	320	1.7	–	20
Run-of-river Hydropower	1000	1000	1000	1000	2.5	0.005	40
Reservoir Hydropower	1700	1700	1700	1700	2.5	0.005	40
PEM Electrolyzer	800	500	400	350	3	–	10
Li-ion Batteries	311	175	153	131	2.5	–	15

[a] Onshore wind turbine values correspond to a reference turbine (capacity: 4.2 MW, rotor diameter: 136 m, hub height 120 m, avg. wind speed: 6.7 m/s) forming the basis for the optimized turbine designs.

Table 4
The average estimates of groundwater sustainable yield in the selected region for 2020 (2015–2035), 2030 (2015–2045) and 2050 (2036–2065) considering two climate scenarios: RCP2.6 and RCP8.5 under conservative, medium, and extreme conditions.

Scenario	Groundwater sustainable yield [mm yr^{-1}]					
	2020		2030		2050	
	RCP2.6	RCP8.5	RCP2.6	RCP8.5	RCP2.6	RCP8.5
Conservative	5.5	3.4	3.1	2.1	0.2	0
Medium	63.3	49.6	49.3	38.3	29.6	19.5
Extreme	150	120.6	122.2	100.9	82.8	54

To mitigate concerns about missing or insufficient data during both data selection and subsequent analysis, a robust approach was adopted, involving the collection and cross-checking of data from diverse sources. This approach ensured that the data used were not only the most reliable but also the most representative of the conditions in the regions studied. The datasets included historical records and single data points from sources such as the World Bank, the International Energy Agency, national statistical offices, and key studies on energy access and employment in Africa [139,140]. The selection process encompassed compiling single data points and historical records within the African context to ensure the most reliable data for the chosen indicators.

2.5.1. Mapping energy access
The indicator for access to energy began with the recognition that data on energy access is typically available only at the national level for both urban and rural areas [140]. By leveraging population density data, urbanization could be defined. To ascertain the regional distribution of the population without access to energy, a correlation between density and access was established for each GID_2 region and validated using data from Ref. [139]:

$$I_1 = \left(EAu^{GID-1} * \sum_{GID\_2} PoPu + EAr^{GID-1} * \sum_{GID\_2} PoPr \right) \Big/ Area \qquad (3)$$

This distribution was calculated using the urban energy access rate at the GID_1 level (EAu^{GID-1}), the rural energy access rate at the GID_1 levels (EAr^{GID-1}), combined with the total urban and rural population per area at the GID_2 level (PoPu and PoPr respectively).

2.5.2. Mapping local employment
Employment figures were calculated using regional multipliers for various renewable energy and power-to-hydrogen technologies. The unemployment rate multiplied by the regional labor force available in GID_2 regions was used to calculate employment for the area, as described by Eq. (4):

$$I_2 = RM * (\ EFRESaverage + EF_{PtH}\ ) * UP * Labor \ / \ Area \qquad (4)$$

Here, RM is the regional multiplier, EFRESaverage represents the global average employment factor for various renewable energy sources, including wind, solar, and hydro, and EF$_{PtH}$ *representing the global employment* factor for power-to-hydrogen technologies. The product is then multiplied by UP (unemployment rate) and Labor (total labor force, i.e., the population between the ages of 15 and 64).

2.5.3. Other impacts
The methodology for calculating the population using traditional biomass mirrored that used for mapping energy access but utilized clean fuel access numbers instead [140]. Regarding the poverty indicator, the share of the population under the poverty line for GID_22 regions was considered, like GID_1 regions [141].

2.5.4. Normalization and weighting
Various normalization techniques, as per OECD guidelines [138],

were applied to the set of indicators. Standardization (or z-scores) was found to best reflect the indicator scores. Equal weighting was applied to direct effects, with less importance given to the indirect ones, justified by the absence of other known means of weighting [142]. Arithmetic means were used for aggregating various composite indicators and sub-indexes.

2.6. Result dissemination via web-based geographical user interface

To ensure widespread accessibility of the study's findings, we developed a user-friendly GUI as a web application which can be accessed via the following URL: https://africa.h2atlas.de/ [143]. The GUI showcases the obtained results, presenting them on a map through color-coded layers where visualization of various factors influencing the potential of green hydrogen in select regions across Africa is facilitated. Users can also engage with the map interface to delve into the data, enabling them to glean insights that foster comprehension of socio, technical and economic aspects of it.

The GUI architecture leverages Docker-based containerization [144], which facilitates a modular and scalable application structure. The frontend employs React [145] and utilizes the Mapbox API [146] to provide dynamic mapping functionalities, allowing users to explore complex geographical data intuitively. The backend integrates Node.js [147] for server-side operations, paired with a PostgreSQL database enhanced with PostGIS [148]. This setup effectively manages and queries spatial data, supporting advanced spatial queries essential for the study. A reverse proxy via Nginx [149] optimizes deployment and enhances performance by managing traffic efficiently. To accurately handle and display geographic data, we employ various software solutions including Geokit [91], GeoPandas [150], and QGIS [151]. These tools guarantee precise geographic positioning of the data through established standards like EPSG:3857, also referred to as Web Mercator [152], and EPSG:4326, commonly known as WGS84 [153].

This framework guarantees a functional and user-friendly GUI that maintains precise and informative visualizations. It enables effective communication of complex data, enhancing understanding of green hydrogen potential across regions. Through this advanced GUI, stakeholders access crucial data, aiding decisions on sustainable energy development in Sub-Saharan Africa.

3. Case study for selected regions

For showing which results can be obtained with the developed multidisciplinary approach one exemplary region for each type of result was selected. The "Ouémé" region in Benin was chosen to illustrate an exemplary land eligibility and renewable energy simulation approach as well as the water availability and socio-economic assessment. The hydrogen modeling approach is then explained based on an exemplary hypothetical region in order to demonstrate all aspects of interest such as groundwater extraction, seawater desalination, utilization of all types of renewable sources of electricity etc. within a single region.

3.1. Land eligibility assessment for open-field photovoltaic and onshore wind turbines

Fig. 3 displays the distribution of local preferences for buffer values of the land eligibility assessment, specifically for the "Leisure and Camping" criterion, which is one of the 33 criteria mentioned in Table 1. Respondents from twenty-two out of the thirty-one surveyed countries in Sub-Saharan Africa submitted their preferences, represented by dots on the graph. For onshore wind, most countries chose a buffer value that is close to the median, although some countries preferred a higher buffer value, and a few countries chose a lower buffer value. On the other hand, for open-field PV, none of the countries chose values close to the median buffer value. Most countries selected a buffer value lower than the median, with only a few countries choosing a higher buffer value. These
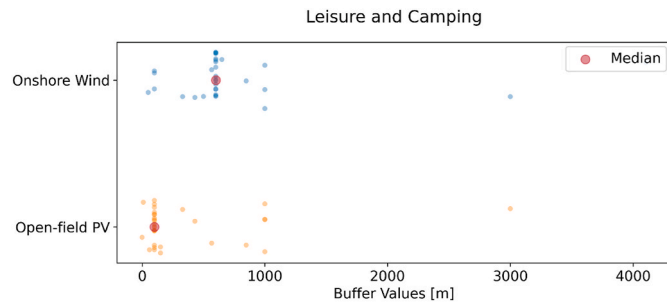
Fig. 3. Distribution of buffer values received for the "Leisure and Camping" criterion from the surveyed countries in Sub-Saharan Africa.

buffer values corresponding to each criterion are applied to all GID_2 regions within a country, unless otherwise stated, and hence also to all regions in Benin including the "Ouémé" region when the final eligibility for the region is be computed.

3.2. Renewable energy potential assessment

Wind turbines and PV modules are placed within the identified exemplary eligible area (based only on three criteria "roads", "settlements" and "forests") which was shown in Fig. 1. Fig. 4 displays the resulting distribution of onshore wind placements and large-scale open-field PV parks. This positioning method has resulted in about 696 eligible locations for the placement of onshore wind turbines for the exemplary region Ouémé (BEN.10_1) in Benin. The total available area for open-field PV placement, after the distribution of polygons, is estimated to be around 318 km^2. This translates to a total capacity of 2.45 GW of onshore wind potential and to approximately 16 GW of open-field PV potential for this specific region.

Fig. 5 displays the distribution of levelized cost of electricity for onshore wind turbines and open-field PV parks across the locations shown in Fig. 4. In the featured region, the cost distribution of electricity generated by onshore wind turbines is relatively steep, ranging from approximately 14 Ct$_€$/kWh to 31 Ct$_€$/kWh. Conversely, electricity produced by distributed open-field PV parks is comparatively inexpensive and has a lower cost spread ranging from ~2.9 Ct$_€$/kWh to 3.1 Ct$_€$/kWh in 2030.
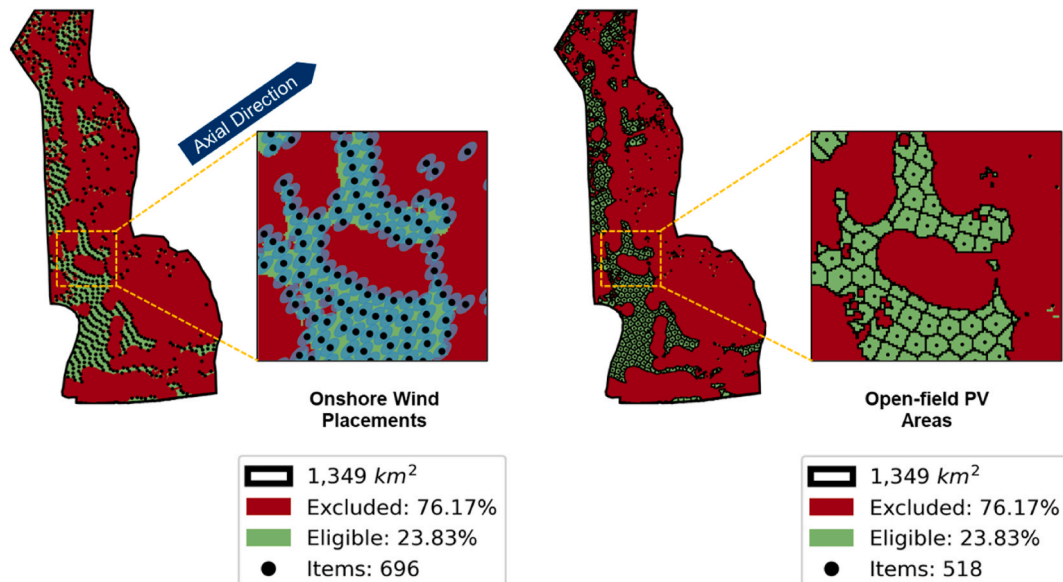
3.3. Sustainable water supply assessment

3.3.1. 2020 groundwater sustainable yield

Reflecting groundwater sustainable yield in 2020, Fig. 6 illustrates long-term average (2015–2035) groundwater sustainable yield maps for the selected region. These maps present two climate scenarios: RCP2.6 (Fig. 6a and c & e) and RCP8.5 (Fig. 6b and d & f). Within each scenario, three cases are investigated: conservative (Fig. 6a and b), medium (Fig. 6c and d), and extreme conditions (Fig. 6e and f). Fig. 6 reveals a noteworthy trend: the availability of water increases progressively from conservative to extreme scenario. As Table 4 shows, the average estimates of 2020 groundwater sustainable yield in the selected region for the year 2020 under RCP2.6 (RCP8.5) scenarios would be 5.5 (3.4) mm yr^{-1} (in the conservative scenario), 63.3 (49.6) mm yr^{-1} (in the medium scenario), and 150 (120.6) mm yr^{-1} (in the extreme scenario). The simulation for the medium case (Fig. 6c and d) positioned between the lower (conservative case) and upper (extreme case) boundaries of available groundwater resources is an ideal and optimum option for hydrogen production.

3.3.2. 2030 groundwater sustainable yield

Long-term average (2015–2045) groundwater sustainable yield maps representative for the year 2030 are shown in Fig. 7, taking into account two climate scenarios: RCP2.6 (Fig. 7a and c & e) and RCP8.5 (Fig. 7b and d & f) and three cases: conservative (Fig. 7a and b), medium (Fig. 7c and d), and extreme conditions (Fig. 7e and f). The regional assessment (Table 4) revealed that across the entire area, the average groundwater sustainable yield for the year 2030 under RCP2.6 (RCP8.5) scenarios would be 3.1 (2.1) mm yr^{-1} (in the conservative scenario), 49.3 (38.3) mm yr^{-1} (in the medium scenario), and 122.2 (100.9) mm yr^{-1} (in the extreme scenario).

3.3.3. 2050 groundwater sustainable yield

Nonetheless, long-term average (2036–2065) groundwater availability representative for 2050 (Fig. 8) under both RCP2.6 (Fig. 8a and c & e) and RCP8.5 (Fig. 8b and d & f) scenarios experienced a notable decrease across all three cases: conservative (Fig. 8a and b), medium (Fig. 8c and d), and extreme conditions (Fig. 8e and f), in comparison to 2020 (Figs. 6) and 2030 (Fig. 7). On average, as indicated in Table 4, the entire region is projected to demonstrate 2050 mean groundwater sustainable yield values under RCP2.6 (RCP8.5) scenarios equal to 0.2 (0) mm yr^{-1} (in the conservative scenario), 29.6 (19.5) mm yr^{-1} (in the

Fig. 4. Distribution of onshore wind turbines (left) and PV area (right) placements within the eligible areas.
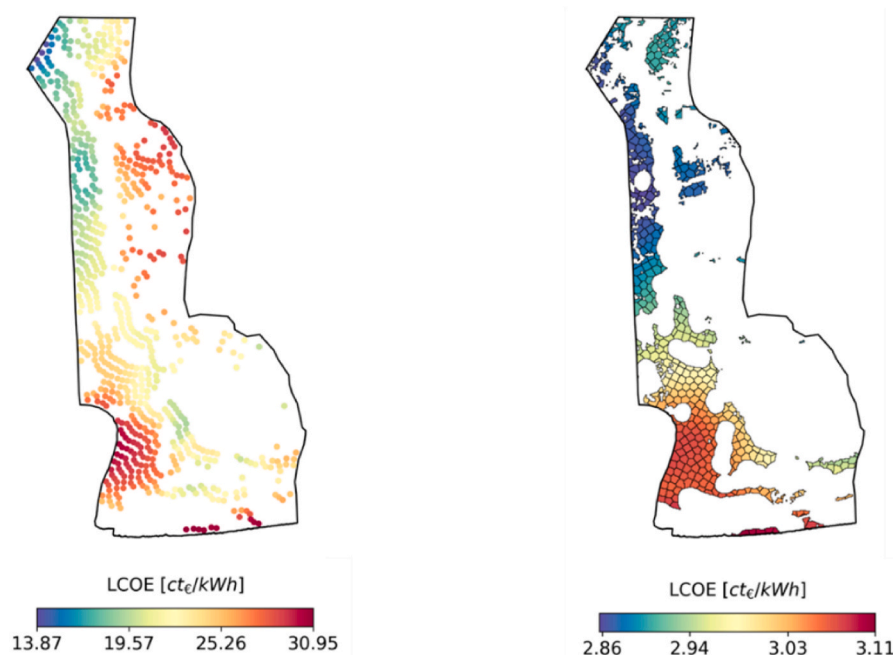
Fig. 5. Levelized cost of electricity (LCOE) for the exemplary onshore wind placements (left) and open-field PV placements (right) corresponding to assumptions for the year 2030.

medium scenario), and 82.8 (54) mm yr^{-1} (in the extreme scenario) which are significantly lower than those observed in 2020 and 2030.

3.4. Local green hydrogen potential assessment

The levelized cost of hydrogen (LCOH) and the respective hydrogen production potential for each analyzed expansion step in an example region in 2050 is shown in Fig. 9. For this step, a hypothetical region was defined that demonstrates all aspects of interest, in particular realistic shares of potentials for all selected technologies except geothermal power and an existing yet limited sustainable groundwater availability. The region has a maximum technical hydrogen potential of 2391 kt$_{H2}$/a, with 50% of the hydrogen being producible from local groundwater (see grey line in Fig. 9). The optimized energy system composition resulting from the cost contribution of the different technologies involved is displayed in the form of a bar at each expansion step. At lower levels of exploitation of the maximum potential, up to about 2%, the electricity required for the hydrogen production is supplied by hydropower (reservoir). Starting from the 4% expansion step and up until the 90% expansion step, in addition to hydropower gradually more and more open-field PV capacity is utilized. Starting from the 96% expansion step, gradually increasing amounts of onshore wind capacity as well as batteries are added to the mix until the 100% expansion step is reached. This shows that onshore wind is the most expensive option to produce hydrogen in this region and additionally requires battery storage.

The LCOH starts at about 1.3 €/kg$_{H2}$ for pure hydropower production and lies at that value up until the 4% expansion step. Including open-field PV into the system increases the LCOH to roughly 2.1 €/kg$_{H2}$, while utilizing onshore wind drives the LCOH gradually to about 2.4 €/kg$_{H2}$ at the 100% expansion step. Below 50% of the maximum potential, local groundwater is used for hydrogen production. Above that, desalination must be used to provide freshwater for the electrolysis. The cost of water supply is negligible though, representing less than 1.2% of the total levelized cost of hydrogen despite the partial use of desalination.

3.5. Socio-economic impact assessment

Here again, the example of Ouémé in Benin is chosen to illustrate the methodology used for the socio-economic impact assessment as shown in Fig. 10. It shows how the results are synthesized at GID_2 regions resolution to assess a socio-economic indicator evaluating the local impact of projects, ranging from very low to very high. Initially, population density at a 1 km resolution is employed to differentiate between urban and rural densities through the urbanization rate. This differentiation is used to determine the population lacking access to energy, including electricity and clean fuel, at a 1 km resolution, utilizing rural and urban access rates at the regional level, and national level if regional data is unavailable. Subsequently, these findings are aggregated at the GID_2 grid to establish the population density without access to electricity per administrative grid area.

The macroeconomic impact is derived from labor density, which is computed from the same urban and rural population densities, adjusted by the average available labor force and unemployment rate at the regional or national level. For Ouémé, the labor force percentage fluctuates between 52% and 58%, with a corresponding regional unemployment rate of 1.6%. This is then multiplied by the regional average employment factor for various technologies. For instance, in the GID_1 region of Fig. 10, this translates to 5.1 jobs/MWp for PV, 3.2 jobs/MWp for onshore wind, 5.9 jobs/MWp for hydro, and 1.7 jobs/MWp for P2H. Additionally, the percentage of population below the poverty line in the region corresponds to an aggregated average of 52 %. This is incorporated in addition to the macroeconomic effects and energy access indicators using a weighted average approach.

4. Conclusions

By utilizing a multidisciplinary approach to cover all crucial dimensions of green hydrogen in Sub-Saharan Africa, robust decision support can be provided. This stems not only from the combination of tools but also from the advances contained in each step. This ranges from the first systematic inclusion of local preferences for land eligibility for renewable energy technologies in Sub-Saharan Africa combined with the best available land cover data and the high level of detail in the
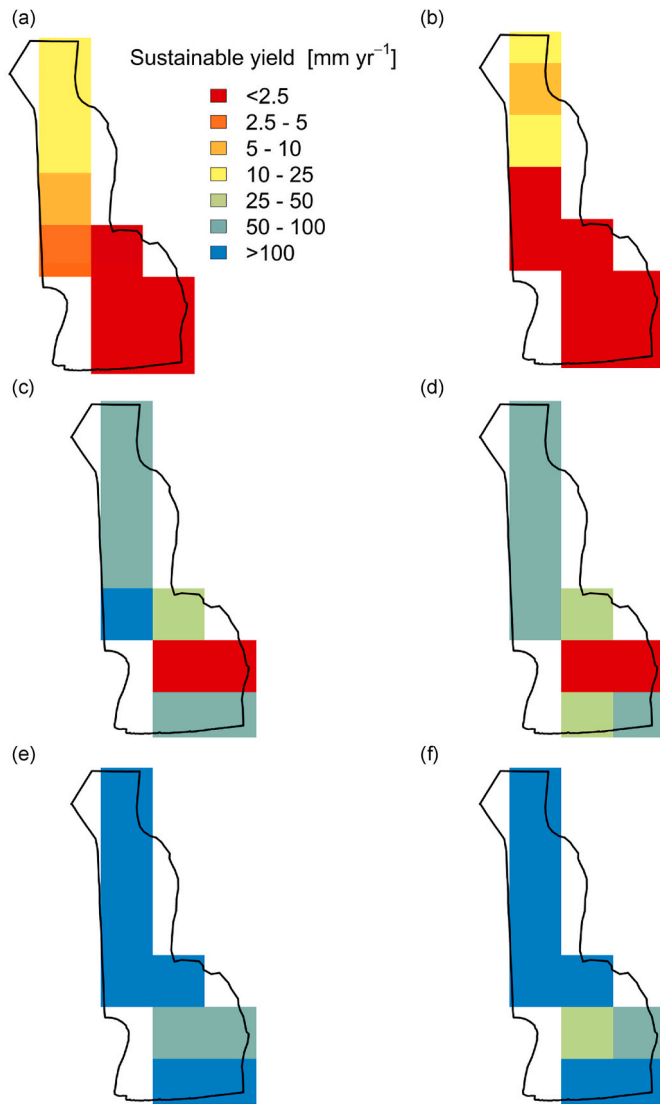
Fig. 6. Groundwater sustainable yield representative for the year 2020 calculated as the long-term average (2015–2035) of simulations, taking into account two climate scenarios: RCP2.6 (a & c & e) and RCP8.5 (b & d & f). Within each scenario, three cases are investigated: conservative (a & b), medium (c & d), and extreme conditions (e & f).
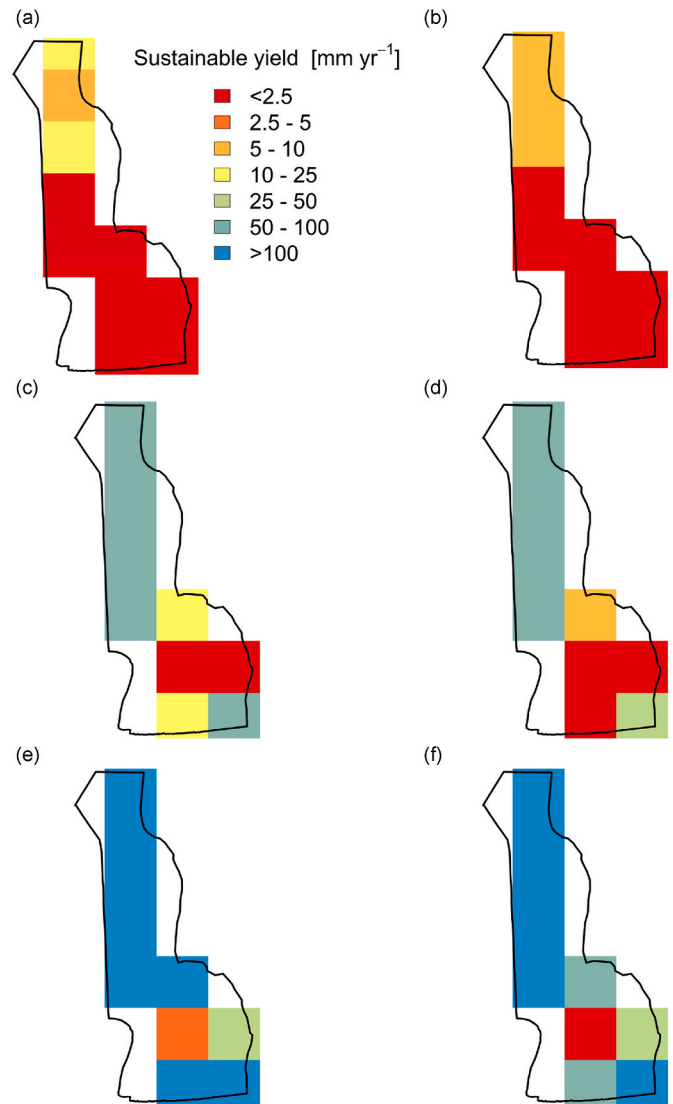

Fig. 7. Groundwater sustainable yield representative for the year 2030 calculated as the long-term average (2015–2045) of simulations, taking into account two climate scenarios: RCP2.6 (a & c & e) and RCP8.5 (b & d & f). Within each scenario, three cases are investigated: conservative (a & b), medium (c & d), and extreme conditions (e & f).

renewable energy potential assessment with specific placements, to the achieved advances in calculating sustainable groundwater yields under different climate scenarios together with considering seawater desalination with water transport for regions without or not sufficient sustainable groundwater yield. Finally, those advances feed-in the new approach to derive the green hydrogen potentials locally with highly resolved optimizing energy system models, which consider the variable nature of the involved renewable energy technologies and their interplay with the other components within the energy system, especially the sizing of electrolysis and batteries. This techno-economic approach under environmental constraints is complemented with a social perspective to enrich the decision support. Each of those steps bear unique advances and options for future applications and improvements.

For the comprehensive land eligibility approach, we used 33 criteria with a high spatial resolution to determine eligible land areas for onshore wind and open field PV. In coordination with local partners in these regions, we determined their local preferences for exclusions. Based on averaged values, we found that local preferences of land eligibilities and their buffer distances can vary between −100% and +1000%. Therefore, it is important to consider the local sociopolitical

preferences to be able to conduct accurate land eligibility analysis.

The approach for the open field PV and onshore wind power for countrywide potential assessment utilizes location specific placements and simulations of PV parks and wind turbines. It can be found that the cost of renewable energies and their range varies between 14 Ct$_€$/kWh to 31 Ct$_€$/kWh for wind power and ~2.9 Ct$_€$/kWh to ~3.1 Ct$_€$/kWh for PV within the exemplary region in Benin. It is also shown that the potentials vary largely within each region. Therefore, a detailed location specific approach as described in this work is necessary to determine the renewable energy potential in the context of hydrogen potential analysis.

Groundwater availability and cost are considered quantitatively at regional scale for the first time in an energy system model and the maximum sustainable shares of groundwater and additionally required freshwater from desalination are calculated. Utilizing land surface modeling stands as a viable avenue to assess water balance elements, compute groundwater recharge, and generate maps depicting groundwater sustainable yield. This sustainable yield essentially denotes the remaining water volume after accounting for all existing human
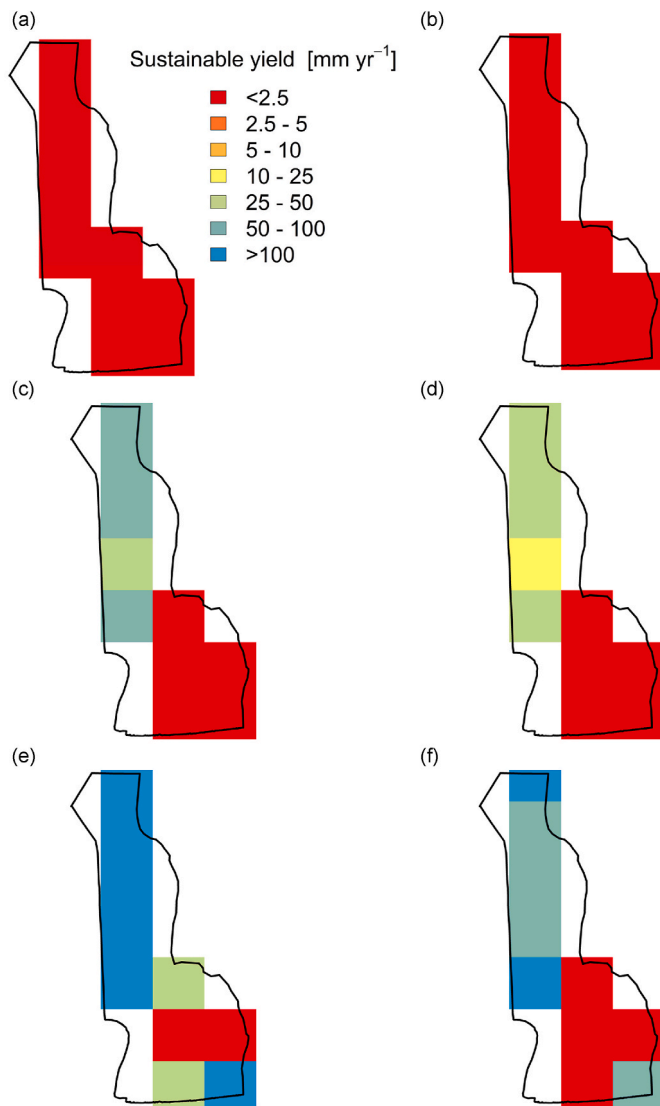
Fig. 8. Groundwater sustainable yield representative for the year 2050 calculated as the long-term average (2035–2065) of simulations, taking into account two climate scenarios: RCP2.6 (left panels) and RCP8.5 (right panels). Within each scenario, three cases are investigated: conservative (a & b), medium (c & d), and extreme conditions (e & f).

Fig. 9. Cost shares of each technology at each expansion step within the hypothetical region for 2050.

requirements and potential environmental water needs. Therefore, these quantitative representations serve as valuable information for evaluating the sustainability of African groundwater resources, offering insights not only into current conditions but also potential scenarios under future climate change projections. As advancements in hydrological modeling continue to evolve and interdisciplinary approaches gain traction, future groundwater analysis may increasingly rely on integrated sub-surface-surface-atmosphere models incorporating real-time data streams from in situ and satellite observations and utilizing machine learning algorithms to enhance predictive capabilities and improve the sustainable management of groundwater resources.

The inclusion of water limitations in the energy system approach shows, that cost of water supply proves negligible in the overall Levelized Cost of Hydrogen (LCOH), which ranges from roughly 1.3 €/kg$_{H2}$ to 2.4 €/kg$_{H2}$ in 2050. Still, careful consideration must be given to the selection of water sources, with options ranging from seawater to groundwater. It should be highlighted that this analysis assumes dry cooling based on Holst et al. [154]. Depending on the selected cooling process, additional water demand for electrolysis may incur, then leading to a total water demand of 17.5–95 l$_{H2O}$/kg$_{H2}$ [155–157].
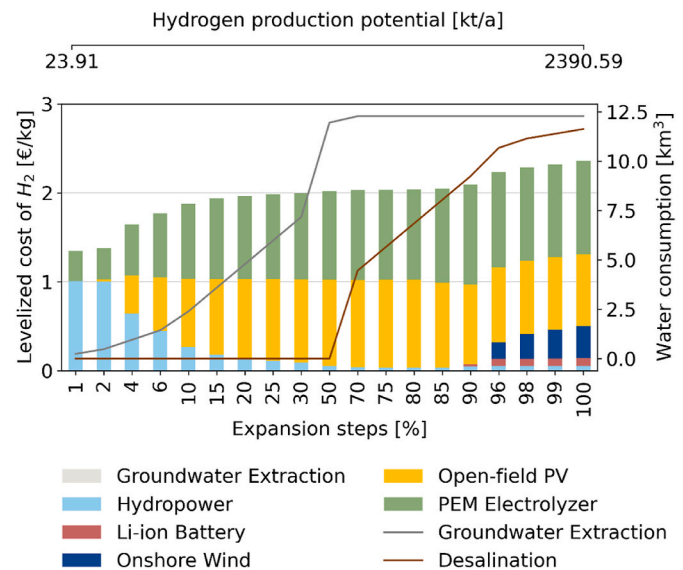
Moreover, this study focuses on local energy systems for hydrogen production. Therefore, synergies between neighboring regions are neglected compared to Franzmann et al. [28].

Regarding the socio-economic dimension of green hydrogen in Sub-Saharan Africa the utilization of the OECD checklist for constructing composite indicators ensured a robust research approach, providing clear direction by focusing on sustainable development goals (SDGs) influenced by green hydrogen projects. This is done based on the analysis of direct and indirect impacts of green hydrogen projects on various SDGs, coupled with spatial data analysis, which enhanced the understanding of socio-economic indicators' feasibility and relevance. Moreover, the integration of local visions through surveys added depth to the Sub-Saharan African vision regarding the socio-economic indicators that should be prioritized. This is ensured by cross-checking from diverse and local sources as well to complete the data collection and mitigate concerns about missing or insufficient data, ensuring reliability. Through this approach the local impact of green hydrogen and renewable energy sources projects are considered for the first time at the regional scale in the Sub-Saharan African case. This is based on macroeconomic effects measured by the direct local employment of potential projects and the indirect promotion of access to electricity and energy via the direct use of renewable energy sources. The main driver of local impact lies in promoting energy access and employing regional labor for construction and operations. The analysis was based on literature comparison to validate the robustness of the results. Thus, the values derived from our study were consistent with those reported in similar studies, further confirming the accuracy and relevance of the chosen indicators and methods. For example, the energy access indicator was based on both national and regional aggregation of population without access to energy [139,140], providing a detailed analysis of energy access disparities in sub-Saharan Africa. Similarly, the employment impact figures were regional adapted based on global employment factors in agreement with the findings of Rutovitz et al. [158], which highlights the impact of different renewable energy technologies on direct job creation. Although the approach uses reliable region-specific data, long-term considerations including the growth of regional renewable industries, necessitates future data improvements to account for broader job and local impacts, such as those induced from infrastructure, manufacturing and export projects associated to a green hydrogen economy.

This study addresses the existing gaps in the literature by presenting a detailed multi-disciplinary methodological framework for assessing the potential for green hydrogen in Sub-Saharan African regions. What
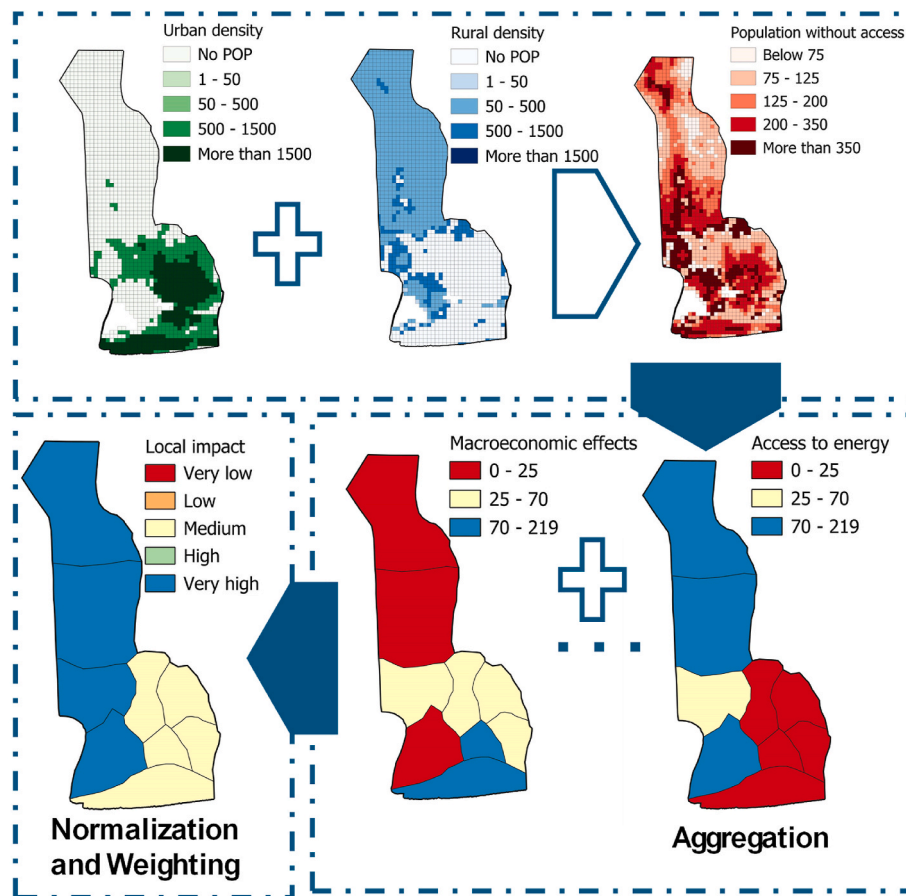
Fig. 10. Example of Ouémé for the construction of the socio-economic local impact indicator.

makes this study unique is its thorough incorporation of land eligibility analysis with consideration of local stakeholder preferences, precise placement of PV and wind parks, high-fidelity hourly energy output simulations from solar and wind resources, co-optimization of solar and wind resources for green hydrogen production, the integration of sustainable groundwater and desalinated seawater provision and considering the socio-economic dimension.

Finally, the results achieved for the case study regions not only prove the applicability of the newly developed approach presented in this paper but the benefits arising from the multidisciplinary approach, too. Those stretch from the value of local preferences for placing renewable energies across endogenous consideration of sustainable water supply to finally identifying main drivers of local socio-economic impacts of green hydrogen. Now a large-scale application will be the next logical step.

CRediT authorship contribution statement

S. Ishmam: Writing – review & editing, Writing – original draft, Visualization, Methodology. **H. Heinrichs:** Writing – review & editing, Writing – original draft, Supervision, Project administration, Methodology, Funding acquisition, Conceptualization. **C. Winkler:** Writing – review & editing, Writing – original draft, Methodology. **B. Bayat:** Writing – review & editing, Writing – original draft, Visualization, Methodology. **A. Lahnaoui:** Writing – review & editing, Writing – original draft, Visualization, Methodology. **S. Agbo:** Writing – review & editing, Writing – original draft, Project administration, Funding acquisition. **E.U. Pena Sanchez:** Writing – review & editing, Writing – original draft, Visualization, Methodology. **D. Franzmann:** Writing – review & editing, Writing – original draft, Visualization, Methodology. **N. Oijeabou:** Writing – review & editing, Methodology. **C. Koerner:** Writing – review & editing, Writing – original draft, Methodology. **Y. Michael:** Writing – review & editing, Writing – original draft, Methodology. **B. Oloruntoba:** Writing – review & editing, Writing – original draft, Methodology. **C. Montzka:** Writing – review & editing, Writing – original draft, Methodology. **H. Vereecken:** Writing – review & editing, Writing – original draft, Methodology. **H. Hendricks Franssen:** Writing – review & editing, Writing – original draft, Methodology. **J. Brendt:** Writing – review & editing, Project administration. **S. Brauner:** Writing – review & editing, Methodology. **W. Kuckshinrichs:** Writing – review & editing, Methodology. **S. Venghaus:** Writing – review & editing, Methodology. **D. Kone:** Writing – review & editing, Project administration. **B. Korgo:** Writing – review & editing, Project administration. **K. Ogunjobi:** Writing – review & editing, Project administration. **V. Chiteculo:** Writing – review & editing, Project administration. **J. Olwoch:** Writing – review & editing, Project administration. **Z. Getenga:** Writing – review & editing, Project administration. **J. Linßen:** Writing – review & editing, Supervision. **D. Stolten:** Writing – review & editing, Supervision.

Declaration of competing interest

The authors declare that they have no known competing financial interests or personal relationships that could have appeared to influence the work reported in this paper.

Acknowledgements

References

[1] Meng X, Gu A, Wu X, Zhou L, Zhou J, Liu B, Mao Z. Status quo of China hydrogen strategy in the field of transportation and international comparisons. Int J Hydrogen Energy 2021;46:28887–99. https://doi.org/10.1016/j.ijhydene.2020.11.049.

[2] Noussan M, Raimondi PP, Scita R, Hafner M. The role of green and blue hydrogen in the energy transition—a technological and geopolitical perspective. Sustainability 2021;13(298). https://doi.org/10.3390/su13010298.

[3] European Commission. A hydrogen strategy for a climate-neutral Europe. European Commission. https://energy.ec.europa.eu/system/files/2020-07/hydrogen_strategy_0.pdf; 2020.

[4] US DOE. Department of energy. U.S. national clean hydrogen strategy and roadmap 2023. https://www.hydrogen.energy.gov/docs/hydrogenprogramlibraries/pdfs/us-national-clean-hydrogen-strategy-roadmap.pdf.

[5] BMWK. Fortschreibung der Nationalen Wasserstoffstrategie. Bundesministerium für Wirtschaft und Klimaschutz. https://www.bmwk.de/Redaktion/DE/Wasserstoff/Downloads/Fortschreibung.html; 2023.

[6] ECREEE. ECOWAS green hydrogen policy and strategy framework. ECOWAS Centre for Renewable Energy and Energy Efficiency (ECREEE) 2023. http://www.ecreee.org/sites/default/files/documents/basic_page/ecowas_green_hydrogen_policy_21112023.pdf.

[7] Burgess J. Kenya launches green hydrogen strategy and road map with EU. S&P Global 2023. https://www.spglobal.com/commodityinsights/en/market-insights/latest-news/electric-power/090523-kenya-launches-green-hydrogen-strategy-and-road-map-with-eu.

[8] Pollet B, Pasupathi S, Swart G. Hydrogen South Africa (HySA) systems competence centre: mission, objectives, technological achievements and breakthroughs. Int J Hydrogen Energy 2014;39(2014):3577–96. https://doi.org/10.1016/j.ijhydene.2013.11.116.

[9] DSI. Hydrogen society Roadmap for South Africa 2021. Department of Science and Innovation, South Africa DSI 2021. https://www.dst.gov.za/images/South_African_Hydrogen_Society_RoadmapV1.pdf.

[10] Ministry of Mines and Energy Namibia. Namibia Green hydrogen and derivatives strategy. Ministry of Mines and Energy Namibia 2022. https://gh2namibia.com/gh2_file_uploads/2022/11/Namibia-GH2-Strategy-Rev2.pdf.

[11] Mentis D, Hermann S, Howells M, Welsch M, Siyal SH. Assessing the technical wind energy potential in Africa a GIS-based approach. Renew Energy 2015;83:110–25. https://doi.org/10.1016/j.renene.2015.03.072.

[12] Winkler B, Lemke S, Ritter J, Lewandowski I. Integrated assessment of renewable energy potential: approach and application in rural South Africa. Environ Innov Soc Transit 2017;24:17–31. https://doi.org/10.1016/j.eist.2016.10.002.

[13] Bosch J, Staffell I, Hawkes AD. Temporally-explicit and spatially-resolved global onshore wind energy potentials. Energy 2017;131:207–17. https://doi.org/10.1016/j.energy.2017.05.052.

[14] Pietzcker RC, Stetter D, Manger S, Luderer G. Using the sun to decarbonize the power sector: the economic potential of photovoltaics and concentrating solar power. Appl Energy 2014;135:704–20. https://doi.org/10.1016/j.apenergy.2014.08.011.

[15] Köberle AC, Gernaat DEHJ, van Vuuren DP. Assessing current and future techno-economic potential of concentrated solar power and photovoltaic electricity generation. Energy 2015;89:739–56. https://doi.org/10.1016/j.energy.2015.05.145.

[16] Yushchenko A, de Bono A, Chatenoux B, Kumar Patel M, Ray N. GIS-based assessment of photovoltaic (PV) and concentrated solar power (CSP) generation potential in West Africa. Renew Sustain Energy Rev 2018;81:2088–103. https://doi.org/10.1016/j.rser.2017.06.021.

[17] Kakoulaki G, Kougias I, Taylor N, Dolci F, Moya J, Jäger-Waldau A. Green hydrogen in Europe – a regional assessment: substituting existing production with electrolysis powered by renewables. Energy Convers Manag 2021;228:113649. https://doi.org/10.1016/j.enconman.2020.113649.

[18] Maestre VM, Ortiz A, Ortiz I. Transition to a low-carbon building stock. Techno-economic and spatial optimization of renewables-hydrogen strategies in Spain. J Energy Storage 2022;56:105889. https://doi.org/10.1016/j.est.2022.105889.

[19] Tlili O, Mansilla C, Linßen J, Reuß M, Grube T, Robinius M, André J, Perez Y, Le Duigou A, Stolten D. Geospatial modelling of the hydrogen infrastructure in France in order to identify the most suited supply chains. Int J Hydrogen Energy 2020;45(4):3053–72. https://doi.org/10.1016/j.ijhydene.2019.11.006.

[20] IRENA.. Global. Hydrogen trade to meet the 1.5°C climate goal: Green hydrogen cost and potential 2022. https://www.irena.org/.publications/2022/May/Global-Hydrogen-trade-Cost.

[21] AbouSeada N, Hatem TM. Climate action: prospects of green hydrogen in Africa. Energy Rep 2022;8:3873–90. https://doi.org/10.1016/j.egyr.2022.02.225.

[22] Mulugetta Y, Sokona Y, Trotter PA, Fankhauser S, Omukuti J, Somavilla Croxatto L, Steffen B, Tesfamichael M, Abraham E, Adam J-P, Agbemabiese L, Agutu C, Aklilu MP, Alao O, Batidzirai B, Bekele G, Dagnachew AG, Davidson O, Denton F, Yussuff A. Africa needs context-relevant evidence to shape its clean energy future. Nat Energy 2022;7(11):1015–22. https://doi.org/10.1038/s41560-022-01152-0.

[23] Asare-Addo M. Green hydrogen potential assessment in Ghana: application of PEM electrolysis process and geospatial-multi-criteria approach. Int J Sustain Energy 2023;42(1):1202–25. https://doi.org/10.1080/14786451.2023.2256892.

[24] Bhandari R. Green hydrogen production potential in west Africa – case of Niger. Renew Energy 2022;196:800–11. https://doi.org/10.1016/j.renene.2022.07.052.

[25] Müller LA, Leonard A, Trotter PA, Hirmer S. Green hydrogen production and use in low- and middle-income countries: a least-cost geospatial modelling approach applied to Kenya. Appl Energy 2023;343:121219. https://doi.org/10.1016/j.apenergy.2023.121219.

[26] Ayodele TR, Munda JL. Potential and economic viability of green hydrogen production by water electrolysis using wind energy resources in South Africa. Int J Hydrogen Energy 2019;44(33):17669–87. https://doi.org/10.1016/j.ijhydene.2019.05.077.

[27] Gado MG, Nasser M, Hassan H. Potential of solar and wind-based green hydrogen production frameworks in African countries. Int J Hydrogen Energy 2024;68:520–36. https://doi.org/10.1016/j.ijhydene.2024.04.272.

[28] Franzmann D, Heinrichs H, Lippkau F, Addanki T, Winkler C, Buchenberg P, Hamacher T, Blesl M, Linßen J, Stolten D. Green hydrogen cost-potentials for global trade. Int J Hydrogen Energy 2023;48(85):33062–76. https://doi.org/10.1016/j.ijhydene.2023.05.012.

[29] Mukelabai MD, Wijayantha UKG, Blanchard RE. Renewable hydrogen economy outlook in Africa. Renew Sustain Energy Rev 2022;167:112705. https://doi.org/10.1016/j.rser.2022.112705.

[30] Beswick RR, Oliveira AM, Yan Y. Does the green hydrogen economy have a water problem? ACS Energy Lett 2021;6(9):3167–9. https://doi.org/10.1021/acsenergylett.1c01375.

[31] Nkiaka E, Bryant RG, Okumah M, Gomo FF. Water security in sub-Saharan Africa: understanding the status of sustainable development goal 6. WIREs Water 2021;8(6):e1552. https://doi.org/10.1002/wat2.1552.

[32] Altchenko Y, Awulachew SB, Brida B, Diallo HA, Mogbante D, Pavelic P, Tindimugaya C, Villholth KG. Management of ground water in Africa including transboundary aquifers: implications for food security, livelihood and climate change adaptation. https://hal.science/hal-02329787/; 2011.

[33] Adelana SM, MacDonald AM. Groundwater research issues in Africa. Applied Groundwater Studies in Africa 2008:11–8.

[34] Calow RC, MacDonald AM, Nicol AL, Robins NS. Ground water security and drought in Africa: linking availability, access, and demand. Ground Water 2010;48(2):246–56. https://doi.org/10.1111/j.1745-6584.2009.00558.x.

[35] Döll P, Fiedler K. Global-scale modeling of groundwater recharge. Hydrol Earth Syst Sci 2008;12(3):863–85.

[36] MacDonald AM, Bonsor HC, Dochartaigh BÉÓ, Taylor RG. Quantitative maps of groundwater resources in Africa. Environ Res Lett 2012;7(2):024009.

[37] UNEP. "Africa water atlas". Division of early warning and assessment (DEWA). United Nations Environment Programme (UNEP) Nairobi, Kenya 2010.

[38] Bierkens MF, Wada Y. Non-renewable groundwater use and groundwater depletion: a review. Environ Res Lett 2019;14(6):63002.

[39] Custodio E. Aquifer overexploitation: what does it mean? Hydrogeol J 2002;10(2):254–77. https://doi.org/10.1007/s10040-002-0188-6.

[40] de Graaf IE, Gleeson T, Van Beek LPH, Sutanudjaja EH, Bierkens MF. Environmental flow limits to global groundwater pumping. Nature 2019;574(7776):90–4.

[41] Rohde M, Matsumoto S, Howard J, Liu S, Riege L, Remson EJ. Groundwater dependent ecosystems under the sustainable groundwater management act. Nat Conserv 2018. https://acwi.gov/swrr/p&p_library/May_2018/18_rohde_%202_tnc_gde_guidance_presentation_swrr_may_2018.pdf.

[42] Alley WM, Leake SA. The journey from safe yield to sustainability. Ground Water 2004;42(1):12–6. https://doi.org/10.1111/j.1745-6584.2004.tb02446.x.

[43] Fetter CW. The concept of safe groundwater yield in coastal AQUIFERS1. JAWRA Journal of the American Water Resources Association 1972;8(6):1173–6. https://doi.org/10.1111/j.1752-1688.1972.tb05259.x.

[44] Fetter CW. Applied hydrogeology" text book 4th Ed. New York: Macmillan College; 2001.

[45] Freeze RA. Three-dimensional, transient, saturated-unsaturated flow in a groundwater basin. Water Resour Res 1971;7(2):347–66. https://doi.org/10.1029/WR007i002p00347.

[46] Kalf FRP, Woolley DR. Applicability and methodology of determining sustainable yield in groundwater systems. Hydrogeol J 2005;13(1):295–312. https://doi.org/10.1007/s10040-004-0401-x.

[47] Shi F, Chi B, Zhao C, Yang T, de la Paix MJ, Lu Y, Gao S. Identifying the sustainable groundwater yield in a Chinese semi-humid basin. J Hydrol 2012;452:14–24.

[48] Sophocleous M. From safe yield to sustainable development of water resources—the Kansas experience. J Hydrol 2000;235(1–2):27–43.

[49] Sophocleous M, Perkins SP. Methodology and application of combined watershed and ground-water models in Kansas. J Hydrol 2000;236(3–4):185–201.

[50] Gleeson T, Cuthbert M, Ferguson G, Perrone D. Global groundwater sustainability, resources, and systems in the anthropocene. Annu Rev Earth Planet Sci 2020;48(1):431–63. https://doi.org/10.1146/annurev-earth-071719-055251.

[51] Taylor RG, Scanlon B, Döll P, Rodell M, Van Beek R, Wada Y, Longuevergne L, Leblanc M, Famiglietti JS, Edmunds M, Konikow L, Green TR, Chen J, Taniguchi M, Bierkens MFP, MacDonald A, Fan Y, Maxwell RM, Yechieli Y, Treidel H. Ground water and climate change. Nat Clim Change 2013;3(4):322–9. https://doi.org/10.1038/nclimate1744.

[52] Healy RW. Estimating groundwater recharge. Cambridge university press 2010.

[53] Scanlon BR, Healy RW, Cook PG. Choosing appropriate techniques for quantifying groundwater recharge. Hydrogeol J 2002;10(1):18–39. https://doi.org/10.1007/s10040-001-0176-2.

[54] MacDonald AM, Lark RM, Taylor RG, Abiye T, Fallas HC, Favreau G, Goni IB, Kebede S, Scanlon B, Sorensen JP. Mapping groundwater recharge in Africa from ground observations and implications for water security. Environ Res Lett 2021;16(3):034012.

[55] L'vovič MI. World water resources and their future. American Geophysical Union; 1979.

[56] Döll P, Lehner B, Kaspar F. Global modeling of groundwater recharge. Proceedings of Third International Conference on Water Resources and the Environment Research, Technical University of Dresden, Germany 2002;1:27–31. https://www.academia.edu/download/41391258/Global_Modeling_of_Groundwater_Recharge20160121-1749-1ljhcbk.pdf.

[57] Alcamo J, Döll P, Henrichs T, Kaspar F, Lehner B, Rösch T, Siebert S. Development and testing of the WaterGAP 2 global model of water use and availability. Hydrol Sci J 2003;48(3):317–37. https://doi.org/10.1623/hysj.48.3.317.45290.

[58] Döll P, Kaspar F, Lehner B. A global hydrological model for deriving water availability indicators: model tuning and validation. J Hydrol 2003;270(1–2):105–34.

[59] Abiye T. Synthesis on groundwater recharge in Southern Africa: a supporting tool for groundwater users. Groundwater for Sustainable Development 2016;2:182–9.

[60] Xu Y, Beekman HE. Groundwater recharge estimation in southern Africa (vol. 64). Unesco. https://unesdoc.unesco.org/ark:/48223/pf0000132404; 2003.

[61] Edmunds WM, Wright EP. Groundwater recharge and palaeoclimate in the Sirte and Kufra basins, Libya. J Hydrol 1979;40(3–4):215–41.

[62] Guendouz A, Moulla AS, Edmunds WM, Zouari K, Shand P, Mamou A. Hydrogeochemical and isotopic evolution of water in the Complexe Terminal aquifer in the Algerian Sahara. Hydrogeol J 2003;11(4):483–95. https://doi.org/10.1007/s10040-003-0263-7.

[63] Sturchio NC, Du X, Purtschert R, Lehmann BE, Sultan M, Patterson LJ, Lu Z-T, Müller P, Bigler T, Bailey K, O'Connor TP, Young L, Lorenzo R, Becker R, El Alfy Z, El Kaliouby B, Dawood Y, Abdallah AMA. One million year old groundwater in the Sahara revealed by krypton-81 and chlorine-36. Geophys Res Lett 2004;31(5):2003GL019234. https://doi.org/10.1029/2003GL019234.

[64] Edmunds WM, Gaye CB. Estimating the spatial variability of groundwater recharge in the Sahel using chloride. J Hydrol 1994;156(1–4):47–59.

[65] Favreau G, Cappelaere B, Massuel S, Leblanc M, Boucher M, Boulain N, Leduc C. Land clearing, climate variability, and water resources increase in semiarid southwest Niger: a review. Water Resour Res 2009;45(7):2007WR006785. https://doi.org/10.1029/2007WR006785.

[66] Leblanc MJ, Favreau G, Massuel S, Tweed SO, Loireau M, Cappelaere B. Land clearance and hydrological change in the Sahel: SW Niger. Global Planet Change 2008;61(3–4):135–50.

[67] Leduc C, Favreau G, Schroeter P. Long-term rise in a sahelian water-table: the continental terminal in South-west Niger. J Hydrol 2001;243(1–2):43–54.

[68] Ibrahim M, Favreau G, Scanlon BR, Seidel JL, Le Coz M, Demarty J, Cappelaere B. Long-term increase in diffuse groundwater recharge following expansion of rainfed cultivation in the Sahel, West Africa. Hydrogeol J 2014;22(6):1293–305. https://doi.org/10.1007/s10040-014-1143-z.

[69] Sami K, Hughes DA. A comparison of recharge estimates to a fractured sedimentary aquifer in South Africa from a chloride mass balance and an integrated surface-subsurface model. J Hydrol 1996;179(1–4):111–36. https://doi.org/10.1016/0022-1694(95)02843-9.

[70] Scanlon BR, Reedy RC, Stonestrom DA, Prudic DE, Dennehy KF. Impact of land use and land cover change on groundwater recharge and quality in the southwestern US. Global Change Biol 2005;11(10):1577–93. https://doi.org/10.1111/j.1365-2486.2005.01026.x.

[71] Siddik MS, Tulip SS, Rahman A, Islam Md N, Haghighi AT, Mustafa SMT. The impact of land use and land cover change on groundwater recharge in northwestern Bangladesh. J Environ Manag 2022;315:115130. https://doi.org/10.1016/j.jenvman.2022.115130.

[72] Bayat B, Oloruntoba B, Montzka C, Vereecken H, Hendricks Franssen H-J. Implications for sustainable water consumption in Africa by simulating five decades (1965–2014) of groundwater recharge. J Hydrol 2023;626:130288. https://doi.org/10.1016/j.jhydrol.2023.130288.

[73] del Río P, Burguillo M. An empirical analysis of the impact of renewable energy deployment on local sustainability. Renew Sustain Energy Rev 2009;13(6):1314–25. https://doi.org/10.1016/j.rser.2008.08.001.

[74] Zhou P, Ang BW, Poh KL. A mathematical programming approach to constructing composite indicators. Ecol Econ 2007;62(2):291–7.

[75] Borbonus S. Generating socio-economic values from renewable energies. Institute for Advanced Sustainability Studies (IASS): Postdam, Germany 2017;32.

[76] Kelly JA, Clinch JP, Kelleher L, Shahab S. Enabling a just transition: a composite indicator for assessing home-heating energy-poverty risk and the impact of environmental policy measures. Energy Pol 2020;146:111791.

[77] Zhang T, Shi X, Zhang D, Xiao J. Socio-economic development and electricity access in developing economies: a long-run model averaging approach. Energy Pol 2019;132:223–31. https://doi.org/10.1016/j.enpol.2019.05.031.

[78] Casati P, Moner-Girona M, Khaleel SI, Szabo S, Nhamo G. Clean energy access as an enabler for social development: a multidimensional analysis for Sub-Saharan Africa. Energy for Sustainable Development 2023;72:114–26.

[79] Zhao J, Dong K, Dong X, Shahbaz M. How renewable energy alleviate energy poverty? A global analysis. Renew Energy 2022;186:299–311.

[80] Lantz TL, Ioppolo G, Yigitcanlar T, Arbolino R. Understanding the correlation between energy transition and urbanization. Environ Innov Soc Transit 2021;40:73–86.

[81] Alstone P, Gershenson D, Kammen DM. Decentralized energy systems for clean electricity access. Nat Clim Change 2015;5(4):305–14.

[82] Mazzucato M, Semieniuk G. Financing renewable energy: who is financing what and why it matters. Technol Forecast Soc Change 2018;127:8–22.

[83] Peña Sánchez EU, Ryberg SD, Heinrichs HU, Stolten D, Robinius M. The potential of variable renewable energy sources in Mexico: a temporally evaluated and geospatially constrained techno-economical assessment. Energies 2021;14(18). https://doi.org/10.3390/en14185779. Article 18.

[84] Ryberg DS. Generation lulls from the future potential of wind and solar energy in Europe. PhD thesis, RWTH Aachen University, 2020.

[85] Global Administrative Areas. GADM database of global administrative areas, version 3.4; 2020. https://gadm.org/.

[86] Deng YY, Haigh M, Pouwels W, Ramaekers L, Brandsma R, Schimschar S, Grözinger J, de Jager D. Quantifying a realistic, worldwide wind and solar electricity supply. Global Environ Change 2015;31:239–52. https://doi.org/10.1016/j.gloenvcha.2015.01.005.

[87] McKenna R, Hollnaicher S, Ostman v. d. Leye P, Fichtner W. Cost-potentials for large onshore wind turbines in Europe. Energy 2015;83:217–29. https://doi.org/10.1016/j.energy.2015.02.016.

[88] Zappa W, van den Broek M. Analysing the potential of integrating wind and solar power in Europe using spatial optimisation under various scenarios. Renew Sustain Energy Rev 2018;94:1192–216. https://doi.org/10.1016/j.rser.2018.05.071.

[89] Ryberg DS, Robinius M, Stolten D. Evaluating land eligibility constraints of renewable energy sources in Europe. Energies 2018;11(5). https://doi.org/10.3390/en11051246. Article 5.

[90] International Renewable Energy Agency. World energy transitions outlook 2023—1.5°C pathway. International Renewable Energy Agency IRENA 2023.

[91] GeoKit. FZJ-IEK3-VSA/geokit: 1.4.0 (Version v1.4.0) [Computer software]. GitHub. https://github.com/FZJ-IEK3-VSA/geokit/tree/v1.4.0; 2024.

[92] GLAES. FZJ-IEK3-VSA/glaes: 1.2.1 (Version v1.2.1) [Computer software]. GitHub. https://github.com/FZJ-IEK3-VSA/glaes/tree/v1.2.1; 2024.

[93] Virtanen P, Gommers R, Oliphant TE, Haberland M, Reddy T, Cournapeau D, Burovski E, Peterson P, Weckesser W, Bright J. Fundamental algorithms for scientific computing in python and SciPy 1.0 contributors. SciPy 1.0. Nat Methods 2020;17:261–72.

[94] GDAL/OGR contributors. GDAL/OGR geospatial data abstraction software library. Open source geospatial foundation. https://doi.org/10.5281/zenodo.5884351; 2024.

[95] Ryberg DS, Caglayan DG, Schmitt S, Linßen J, Stolten D, Robinius M. The future of European onshore wind energy potential: detailed distribution and simulation of advanced turbine designs. Energy 2019;182:1222–38. https://doi.org/10.1016/j.energy.2019.06.052.

[96] Hersbach H, Bell B, Berrisford P, Biavati G, Horányi A, Muñoz Sabater J, Nicolas J, Peubey C, Radu R, Rozum I, others. ERA5 hourly data on single levels from 1979 to present. Copernicus Climate Change Service (C3s) Climate Data Store (Cds) 2018;10(10):24381.

[97] RESKit. FZJ-IEK3-VSA/reskit: 0.3.0 (Version v0.3.0) [Computer software]. GitHub. https://github.com/FZJ-IEK3-VSA/RESKit/tree/v0.3.0; 2024.

[98] Okabe A, Boots B, Sugihara K, Chiu SN. Spatial tessellations: concepts and applications of Voronoi diagrams. 2009.

[99] Mathews D, Ó Gallachóir B, Deane P. Systematic bias in reanalysis-derived solar power profiles & the potential for error propagation in long duration energy storage studies. Appl Energy 2023;336:120819. https://doi.org/10.1016/j.apenergy.2023.120819.

[100] Olauson J. ERA5: the new champion of wind power modelling? Renew Energy 2018;126:322–31. https://doi.org/10.1016/j.renene.2018.03.056.

[101] Frank CW, Wahl S, Keller JD, Pospichal B, Hense A, Crewell S. Bias correction of a novel European reanalysis data set for solar energy applications. Sol Energy 2018;164:12–24. https://doi.org/10.1016/j.solener.2018.02.012.

[102] Staffell I, Pfenninger S. Using bias-corrected reanalysis to simulate current and future wind power output. Energy 2016;114:1224–39. https://doi.org/10.1016/j. energy.2016.08.068.

[103] Staffell I, Pfenninger S. Using bias-corrected reanalysis to simulate current and future wind power output. Energy 2016;114:1224–39. https://doi.org/10.1016/j. energy.2016.08.068.

[104] Tippett MK, Trenary L, DelSole T, Pegion K, L'Heureux ML. Sources of bias in the monthly CFSv2 forecast climatology. J Appl Meteorol Climatol 2018;57(5): 1111–22. https://doi.org/10.1175/JAMC-D-17-0299.1.

[105] Sterl S, Devillers A, Chawanda CJ, van Griensven A, Thiery W, Russo D. A spatiotemporal atlas of hydropower in Africa for energy modelling purposes. Open Research Europe 2021;1.

[106] International Renewable Energy Agency. Renewable power generation costs in 2019 [ISBN 978-92-9260-244-4]. IRENA. https://www.irena.org/-/media/Files/ IRENA/Agency/Publication/2020/Jun/IRENA_Power_Generation_Costs_2019. pdf; 2020.

[107] David Franzmann. Einfluss von regelbarer Stromerzeugung und Speichern auf Energieausfälle in erneuerbaren Energiesystemen, PhD thesis, RWTH Aachen University, 2024, Unpublished.

[108] Aghahosseini A, Breyer C. From hot rock to useful energy: a global estimate of enhanced geothermal systems potential. Appl Energy 2020;279:115769. https:// doi.org/10.1016/j.apenergy.2020.115769.

[109] Goutorbe B, Poort J, Lucazeau F, Raillard S. Global heat flow trends resolved from multiple geological and geophysical proxies. Geophys J Int 2011;187(3):1405–19. https://doi.org/10.1111/j.1365-246X.2011.05228.x.

[110] Augustine C. A methodology for calculating EGS electricity generation potential based on the gringarten model for heat extraction from fractured rock. https: //www.osti.gov/biblio/1357412; 2017 [journal =].

[111] Gringarten AC, Sauty JP. A theoretical study of heat extraction from aquifers with uniform regional flow. 1975.

[112] Tester JW. The future of geothermal energy: impact of enhanced geothermal systems (EGS) on the United States in the 21st century. In: Idaho national laboratory; 2006.

[113] Mines G. GETEM user manual. In: Idaho national laboratory; 2016.

[114] Lawrence DM, Fisher RA, Koven CD, Oleson KW, Swenson SC, Bonan G, Collier N, Ghimire B, Van Kampenhout L, Kennedy D, Kluzek E, Lawrence PJ, Li F, Li H, Lombardozzi D, Riley WJ, Sacks WJ, Shi M, Vertenstein M, Zeng X. The community land model version 5: description of new features, benchmarking, and impact of forcing uncertainty. J Adv Model Earth Syst 2019;11(12):4245–87. https://doi.org/10.1029/2018MS001583.

[115] Sutanudjaja EH, Van Beek R, Wanders N, Wada Y, Bosmans JH, Drost N, Van Der Ent RJ, De Graaf IE, Hoch JM, De Jong K. PCR-GLOBWB 2: a 5 arcmin global hydrological and water resources model. Geosci Model Dev (GMD) 2018;11(6): 2429–53.

[116] Hahn J, Lee Y, Kim N, Hahn C, Lee S. The groundwater resources and sustainable yield of Cheju volcanic island, Korea. Environ Geol 1997;33(1):43–53. https:// doi.org/10.1007/s002540050223.

[117] Meinzer OE. Quantitative method of estimating ground-water supplies. Bull Geol Soc Am 1920;31(2):329–38.

[118] Rossi M, Donnini M, Beddini G. Nationwide groundwater recharge evaluation for a sustainable water withdrawal over Italy. J Hydrol: Reg Stud 2022;43:101172. https://doi.org/10.1016/j.ejrh.2022.101172.

[119] Ozdogan M, Rodell M, Beaudoing HK, Toll DL. Simulating the effects of irrigation over the United States in a land surface model based on satellite-derived agricultural data. J Hydrometeorol 2010;11(1):171–84. https://doi.org/10.1175/ 2009JHM1116.1.

[120] Alley WM, Reilly TE, Franke OL. Sustainability of ground-water resources. U.S. Department of the interior, U.S. Geological survey. 1999.

[121] Maimone M. Defining and managing sustainable yield. Ground Water 2004;42(6): 809–14. https://doi.org/10.1111/j.1745-6584.2004.tb02739.x.

[122] Miles JC, Chambet PD. Safe yield of aquifers. J Water Resour Plann Manag 1995; 121(1):1–8. https://doi.org/10.1061/(ASCE)0733-9496(1995)121:1(1.

[123] Sørland SL, Brogli R, Pothapakula PK, Russo E, Van De Walle J, Ahrens B, Anders I, Bucchignani E, Davin EL, Demory M-E, Dosio A, Feldmann H, Früh B, Geyer B, Keuler K, Lee D, Li D, Van Lipzig NPM, Min S-K, Thiery W. COSMO-CLM regional climate simulations in the Coordinated Regional Climate Downscaling Experiment (CORDEX) framework: a review. Geosci Model Dev (GMD) 2021;14 (8):5125–54. https://doi.org/10.5194/gmd-14-5125-2021.

[124] Coppola E, Stocchi P, Pichelli E, Torres Alavez JA, Glazer R, Giuliani G, Di Sante F, Nogherotto R, Giorgi F. Non-Hydrostatic RegCM4 (RegCM4-NH): model description and case studies over multiple domains. https://doi.org/10.5194/ gmd-2020-435; 2021.

[125] Pietikäinen J-P, Markkanen T, Sieck K, Jacob D, Korhonen J, Räisänen P, Gao Y, Ahola J, Korhonen H, Laaksonen A, Kaurola J. The regional climate model REMO (v2015) coupled with the 1-D freshwater lake model FLake (v1): fenno-Scandinavian climate and lakes. Geosci Model Dev (GMD) 2018;11(4):1321–42. https://doi.org/10.5194/gmd-11-1321-2018.

[126] Gutjahr O, Putrasahan D, Lohmann K, Jungclaus JH, Von Storch J-S, Brüggemann N, Haak H, Stössel A. Max planck institute earth system model (MPI-ESM1.2) for the high-resolution model intercomparison project (HighResMIP). Geosci Model Dev (GMD) 2019;12(7):3241–81. https://doi.org/10.5194/gmd-12-3241-2019.

[127] Bentsen M, Bethke I, Debernard JB, Iversen T, Kirkevåg A, Seland Ø, Drange H, Roelandt C, Seierstad IA, Hoose C, Kristjánsson JE. The Norwegian earth system model, NorESM1-M – Part 1: description and basic evaluation of the physical climate. Geosci Model Dev (GMD) 2013;6(3):687–720. https://doi.org/10.5194/ gmd-6-687-2013.

[128] United Nations ESCWA. ESCWA water development report 3: role of desalination in addressing water scarcity. https://www.unescwa.org/publications/escwa-w ater-development-report-3-role-desalination-addressing-water-scarcity; 2009.

[129] GADM. Database of global administrative areas, version 3.4; 2023. https://gadm. org.

[130] Reuß M, Dimos P, Léon A, Grube T, Robinius M, Stolten D. Hydrogen road transport analysis in the energy system: a case study for Germany through 2050. Energies, 14(11) 2021;3166. https://doi.org/10.3390/en14113166.

[131] OpenTopography. ALOS World 3D - 30m. OpenTopography. https://doi. org/10.5069/G94M92HB; 2016.

[132] Loutatidou S, Chalermthai B, Marpu PR, Arafat HA. Capital cost estimation of RO plants: GCC countries versus southern Europe. Desalination 2014;347:103–11. https://doi.org/10.1016/j.desal.2014.05.033.

[133] Heinrichs H, Winkler C, Franzmann D, Linßen J, Stolten D. Die Rolle von Meerwasserentsalzungsanlagen in einer globalen grünen Wasserstoffwirtschaft. 14. Aachener Tagung Wassertechnologie 2021. https://juser.fz-juelich.de/reco rd/905482.

[134] Welder L, Ryberg DS, Kotzur L, Grube T, Robinius M, Stolten D. Spatio-temporal optimization of a future energy system for power-to-hydrogen applications in Germany. Energy 2018;158:1130–49. https://doi.org/10.1016/j. energy.2018.05.059.

[135] Groß T, Knosall K, Hoffmann M, Pflugtadt N, Stolten D. ETHOS.FINE: a framework for integrated energy system assessment. Submitted to JOSS 2024. https://doi.org/10.48550/arXiv.2311.05930.

[136] Stolten D, Markewitz P, Schöb T, Kullmann F, Risch S, Groß T. Neue Ziele auf alten Wegen? Strategien für eine treibhausgasneutrale Energieversorgung bis zum Jahr 2045. 2021.

[137] Brauner S, Lahnaoui A, Agbo S, Böschen S, Kuckshinrichs W. Towards green hydrogen?–A comparison of German and African visions and expectations in the context of the H2Atlas-Africa project. Energy Strategy Rev 2023;50:101204.

[138] Union E, Centre JR. Handbook on constructing composite indicators: methodology and user guide. OECD publishing. 2008.

[139] Falchetta G, Pachauri S, Byers E, Danylo O, Parkinson SC. Satellite observations reveal inequalities in the progress and effectiveness of recent electrification in sub-Saharan Africa. One Earth 2020;2(4):364–79.

[140] Ritchie H, Roser M, Rosado P. Access to energy. Published online at, OurWorldI nData.Org; 2019.

[141] Dang Hai-Anh H, Cong Nguyen Minh, Trinh Trong-Anh. Global subnational atlas of poverty (version V4). Harvard Dataverse 2022. https://doi.org/10.7910/D VN/MLHFAF.

[142] Ebert U, Welsch H. Meaningful environmental indices: a social choice approach. J Environ Econ Manag 2004;47(2):270–83.

[143] Jülich Systems Analysis, & IBG-3. Forschungszentrum Juelich. H2Atlas-GUI. https://africa.h2atlas.de/; 2024.

[144] Docker. Docker. https://www.docker.com/; 2024.

[145] React. React. https://react.dev/; 2024.

[146] Mapbox. https://www.mapbox.com/; 2024.

[147] Node.js. Node.js. https://nodejs.org/; 2024.

[148] PostGIS. PostGIS. https://postgis.net/; 2024.

[149] Nginx. Nginx. https://www.nginx.com/; 2024.

[150] Van den Bossche Joris, Jordahl Kelsey, Fleischmann Martin, Richards Matt, McBride James, Wasserman Jacob, Garcia Badaracco Adrian, Snow Alan D, Ward Brendan, Tratner Jeff, Gerard Jeffrey, Perry Matthew, Farmer Carson, Hjelle Geir Arne, Taves Mike, Hoeven Ewout ter, Cochran Micah, Bell Ray, rraymondgh, Aleksey Bilogur. geopandas/geopandas: V1.0.0-alpha1 (Version v1.0.0-alpha1) [Computer software]. [object Object]. https://doi.org/10. 5281/ZENODO.2585848; 2024.

[151] QGIS.org. QGIS geographic information system (version 3.18) [computer software]. QGIS association. https://www.qgis.org; 2024.

[152] European Petroleum Survey Group Geodesy. EPSG: 3857 WGS 84. https://epsg. org/crs_3857/WGS-84-Pseudo-Mercator.html; 2020.

[153] European Petroleum Survey Group Geodesy. EPSG: 4326 WGS 84. https://epsg. org/crs_4326/WGS-84.html; 2022.

[154] Holst M, Aschbrenner S, Smolinka T, Voglstätter C, Grimm G. Cost forecast for low temperature electrolysis –technology driven bottom-up prognosis for PEM and alkaline water electrolysis systems. https://www.ise.fraunhofer.de/conten t/dam/ise/de/documents/publications/studies/cost-forecast-for-low-temperatu re-electrolysis.pdf; 2021.

[155] Global Alliance Powerfuels. Water consumption of powerfuels. 2021.

[156] IRENA, & Bluerisk. Water for hydrogen production. International Renewable Energy Agency IRENA 2023.

[157] Kabir MM, Akter Mst M, Huang Z, Tijing L, Shon HK. Hydrogen production from water industries for a circular economy. Desalination 2023;554:116448. https:// doi.org/10.1016/j.desal.2023.116448.

[158] Rutovitz J, Dominish E, Downes J. Calculating global energy sector jobs: 2015 methodology. 2015.